2011

Translational and Rotational Control of an Asteroid Orbiting Satellite

Takahiro Kuhara

TRANSLATIONAL AND ROTATIONAL CONTROL OF AN ASTEROID ORBITING SATELLITE

By

Takahiro Kuhara

A thesis submitted to the Physical Sciences Department

In Partial Fulfillment of the Requirements of

Master of Science in Engineering Physics

Embry-Riddle Aeronautical University

Daytona Beach, FL 32114

Fall 2011

TRANSLATIONAL AND ROTATIONAL CONTROL OF AN ASTEROID ORBITING SATELLITE

By Takahiro Kuhara

This thesis was prepared under the direction of the candidate's thesis committee chair, Dr. Mahmut Reyhanoglu, Department of Physical Sciences, and has been approved by the members of his thesis committee. It was submitted to the Department of Physical Sciences and was accepted in partial fulfillment of the requirements for the Degree of Master of Science in Engineering Physics.

THESIS COMMITTEE:

M. Reyhanoglu

Dr. Mahmut Reyhanoglu, Chair

Dr. Jason Aufdenberg, Member

Dr. Bereket Berhane, Member

Dr. Peter Erdman
MSEP Graduate Program Coordinator

M. Hickey

Dr. Michael Hickey
Department Chair, Physical Sciences

Dr. Robert Oxley
Associate V.P. for Academics

1-6-2012

Date

Abstract

The objective of this thesis is to analyze an effective control scheme for an asteroid orbiting satellite. The thesis first summarizes the progress made in the dynamics formulation of such satellites and then provides a theoretical framework for the control system design. The control objective is to maintain a nadir pointing attitude on a circular equatorial orbit. Using established control design techniques, feedback laws are constructed to control both rotational and translational motion of the satellite so that the control objective is achieved. Computer simulations are carried out to illustrate the effectiveness of the control laws.

Acknowledgments

I am deeply grateful to my advisor, Dr. Mahmut Reyhanoglu for help and guidance during this work. Without his clear and concise explanation, I would have not succeeded in my studies. He kept me pushed and focused on my thesis. I also would like to thank my committee members, Dr. Aufdenberg and Dr. Berhane. I would like to thank professor Timothy McGreevy and the Physical Science department for employing me as a graduate student assistant and providing me with finacial support during my study. I thank my roommate Jun Shishino for keeping me focused on my work. I also thank my knowledgeable and considerate friends, Michael Leaning, Fernando Morita, Thomas Moore, Stephen Armstrong, Eiji Yoshimoto, and Satoshi Yoshimoto. Finally I appreciate my family, Mitsuko Kuhara and Kazuhiro Kuhara for their support and love.

Contents

1 Introduction **1**

1.1 Exploration of Small Solar System Bodies 1

1.2 Analysis of the Orbital and Attitude Dynamics Around a Small Solar System Body 4

1.3 Basic Information on 433 Eros 5

1.4 Contribution of Thesis 7

1.5 Organization of Thesis 7

2 Background on Lyapunov Stability Theory **9**

2.1 Introduction to Lyapunov's Stability Theory 9

2.2 Lyapunov's Second Stability Theorem 12

3 Gravitational Potential Field Model **13**

3.1 Gravitational Potential Approximation 13

3.1.1 Gravitational Potential Field Models 13

3.1.2 MacCullagh's Approximation 15

3.1.3 Spherical Harmonic Gravitational Potential 16

3.2 Gravity-Gradient Torque 19

3.2.1 Coordinate Systems 20

3.2.2 Gravitational Force 24

3.2.3 Gravity-Gradient Torque . . . 25

4 Translational and Rotational Dynamics 27

4.1 Translational Dynamics . . . 27

4.1.1 Equations of Motion . . . 27

4.1.2 Matlab Simulation . . . 30

4.2 Rotational Kinematics and Dynamics . . . 38

4.2.1 Quaternions . . . 38

4.2.2 Reference Frames and Rotations . . . 38

4.2.3 Rotational Kinematics . . . 40

4.2.4 Gravity-Gradient Torque in Terms of Quaternions . . . 43

4.2.5 Rotational Dynamics . . . 44

5 Translational and Rotational Control 47

5.1 Translational Control Law . . . 47

5.2 Matlab Results . . . 50

5.3 Rotational Control Law . . . 58

5.4 Matlab Results . . . 60

6 Conclusions 63

7 Matlab Code 64

7.1 Translational Motion MATLAB Code . . . 64

7.1.1 Uncontrolled Translational Motion . . . 64

7.1.2 Controlled Translational Motion . . . 70

7.2 Rotational Motion MATLAB Code . . . 79

7.2.1 Uncontrolled Rotational Motion . . . 79

7.2.2 Controlled Rotational Motion . . . 84

Bibliography **94**

List of Figures

1.1 Hayabusa landing on the asteroid Itokawa [7]. 3

1.2 433 Eros [11]. 7

2.1 Lyapunov Stable. 11

3.1 Geometry 14

3.2 Position vectors in spherical coordinates. 17

3.3 Inertial frame and orbital frame in equatorial plane 21

3.4 Spacecraft body fixed frame, orbital frame, and asteroid body fixed frame. 21

4.1 Translational motion. 28

4.2 Three dimensional uncontrolled spacecraft motion in the the asteroid frame ($R_c = 50$ km). 32

4.3 Two dimensional uncontrolled spacecraft motion in the asteroid frame ($R_c = 50$ km). 33

4.4 Uncontrolled spacecraft x, y, and z positions ($R_c = 50$ km). 34

4.5 Three dimensional uncontrolled spacecraft motion in the the inertial frame ($R_c = 50$ km). 35

4.6 Two dimensional uncontrolled spacecraft motion in the inertial frame ($R_c = 50$ km). 36

4.7 Uncontrolled spacecraft X, Y, and Z positions (R_c = 50 km). 37
4.8 Direction cosines between a vector $\boldsymbol{r}$ and the frame $\mathcal{F}_o$. 39
4.9 Geometry describing Euler's theorem. 40
4.10 Geometrical interpretation of the rotation matrix. 41
4.11 Quaternions for uncontrolled rotational motion. 46

5.1 Three dimensional controlled spacecraft motion in the the asteroid frame (R_c = 50 km). 51
5.2 Two dimensional controlled spacecraft motion in the asteroid frame (R_c = 50 km). 52
5.3 Controlled spacecraft x, y, and z positions (R_c = 50 km). 53
5.4 Three dimensional controlled spacecraft motion in the the inertial frame (R_c = 50 km). 54
5.5 Two dimensional controlled spacecraft motion in the inertial frame (R_c = 50 km). 55
5.6 Controlled spacecraft X, Y, and Z positions (R_c = 50 km). 56
5.7 Control force F_a. 57
5.8 Quaternions for controlled rotational motion. 61
5.9 Control torque τ. 62

Chapter 1

Introduction

1.1 Exploration of Small Solar System Bodies

Since the Italian astronomer Giuseppe Piazzi initially discovered asteroid Ceres in 1801, more than three hundred thousand asteroids have been found. Asteroids are small solar system bodies and are made of rocks, ice, carbon, or metals. It is claimed that the primary conditions of the chemical structure are relatively well kept in the primitive asteroids in comparison with planets and moons since the asteroids are not large enough to have crustal movement and are not weathered due to the lack of the atmosphere. The clues to the source of the formation of the planets and the conditions of the beginning of the solar system might be obtained once the technology to analyze the asteroids is established. The asteroids are prospective places of mines and human colonization due to their material structure. Asteroids might have materials rare on the Earth. Heavy materials which are expensive to launch from the Earth might be obtained from asteroids and used for the construction of spacecraft or space structures. Some asteroids contain ice on their surfaces. The ice can be a source of oxygen for air conditioning and hydrogen for fuelling space vehicles. In the future, hydrogen might be also used in a nuclear fusion reactor. The orbits of some asteroids pass between the Earth and Moon. This proposes that less energy is needed to reach them than the Moon, which is also a possible source of the colonization and mining. For these reasons, the interest in mission to the asteroids is increasing now.

A number of missions to asteroids and comets have already been operated by several countries. Giotto was launched in 1985 by ESA. It flew by and surveyed Halley's Comet at a distance of 596 kilometers. The detailed shape, size, surface condition, and chemical composition of the Halley's nucleus and its tail were obtained. The Near Earth Asteroid Rendezvous (NEAR) mission was operated by NASA. NEAR Shoemaker which launched in 1996, had researched the asteroids 253 Mathilde and 433 Eros. It orbited Eros for a year at a distance between 20 and 40 kilometers and obtained much information of the geomorphological features. In the end, it landed on Eros successfully serving as a reference for future asteroid mission even though the probe was not designed to do so. Hayabusa 1 was operated between 2003 and 2010 by Japanese Aerospace Exploration Agency (JAXA). It studied 25143 Itokawa, collected samples of the asteroid material, and returned to the Earth. The mission objective of JAXA's Hayabusa 2 is also sample return. In the Hayabusa 2 mission, the probe makes a crater to obtain the inner material of an asteroid, 1999 Ju3. OSIRIS-REx is NASA's sample return mission and also examines the Yarkovsky effect which is caused by the anisotropic emission of thermal photons. These photons have momentum and affect the motion of rotating bodies in space. Sample return missions are valuable because these samples can be analyzed with the latest technology. Analysis by the equipment of the spacecraft is also useful but might be outdated because it takes years to rendezvous with asteroids. Some missions are currently being operated. Rosetta was planned by ESA to have long survey of the comet 46P/Wirtanen, but due to an explosion accident of the Ariane 5 rocket in 2002, the destination was changed to the comet 67P/Churyumov-Gerasimenko. The Rosetta probe was launched in 2004,

Figure 1.1: Hayabusa landing on the asteroid Itokawa [7].

flew by the asteroids 2867 Steins in 2008 and 21 Lutetia in 2010 and is heading to its destination and plans to drop the lander, Philae, onto the comet. The Dawn mission, operated by NASA, was launched in 2007 and is now orbiting the asteroid 4 Vesta and will leave for Ceres in 2012. Through the research on these two different types of asteroids, the mystery of the beginning of the solar system might be understood more deeply. The Dawn probe is scheduled to be the first artificial object to stay forever in the asteroid belt which is the region between the orbits of Mars and Jupiter. ESA's Don Quijote is planned to launch in 2013 or 2015 and its mission is to deflect an asteroid by crashing a spacecraft into the asteroid. Two space probes are used for this mission. One is an orbiter which observes the effect of the impact and the other is an impactor which crashes into the asteroid. This mission examines the possibility of deflecting an asteroid on a collision course with the Earth. Due to the cancellation of the US Constellation program which is a manned space flight program, interest in the exploration of asteroids is increasing. In April 2010 president Obama announced his space vision to send astronauts to an asteroid by 2025 [10].

1.2 Analysis of the Orbital and Attitude Dynamics Around a Small Solar System Body

With the increasing interest in missions to asteroids and comets, the necessity and importance of orbital and attitude dynamics analyses of the small solar system bodies are increasing in order to make these missions successful and useful. A number of papers which examine the orbital and attitude dynamics of spacecrafts around asteroids have been published. Scheeres presented some orbital dynamics about asteroids ([1],[2],[12]) and estimated the parameters of some asteroids such as shape, gravity, density, and rotation state ([5],[3]). Asteroids and comets have usually irregular shapes and this leads to the complicated orbital and attitude dynamics in comparison with approximately spherical bodies such as the Earth. The gravitational potential of the irregular bodies is different from simple spherical bodies. For the irregular bodies, the oblateness and the ellipticity have to be considered in the gravitational potential and these values are dependent upon the shape of the asteroids and the distribution of mass indide the asteroid. The gravitational potential analysis is used in the majority of the papers about the motion of the spacecraft in orbit about an asteroid ([1],[5],[2],[4],[6]). The gravity term C_{22} in the equation of the gravitational potential represents the equatorial ellipticity of the central body. The asteroids and comets have much greater values of C_{22} than that of the planets in the solar system due to their shape. The planets usually have a spherical shape, but the small solar system bodies have irregular shape ([5],[3],[4]). Scheeres showed the effects of the gravity terms C_{20} and C_{30}, which characterize the oblateness of the asteroids and comets ([1],[5],[2]). The oblateness and ellipticity have the same meaning, the aspect ratio of the oblate spheroid. In order to distinguish the equatorial from the polar oblateness, the oblateness is used for the polar plane and the ellipticity is used for the equatorial plane. Spacecrafts are disturbed by several factors such as the solar wind, the magnetic field of the planet, and the gravitational force of the other planets [5]. However these factors are negligibly small in the region close to asteroids. Therefore most papers have assumed that the gravitational potential is the only external force acting on the spacecraft ([1],[4],[9]). The pitch motion of a spacecraft in orbit around 433 Eros was identified by analyzing the equation of motion and the gravitational potential by Misra and Panchenko [9]. The attitude motion of the spacecraft depends heavily on the shape of the asteroid and the rotational state. Lagrange's planetary equations, which state the time derivative of the orbital elements have also been examined to analyze the dynamics ([1],[2],[4],[14]).

1.3 Basic Information on 433 Eros

This thesis presents the orbital and attitude control of a spacecraft around the asteroid 433 Eros. The properties such as the density, the size, and the orbital elements of Eros were obtained by NEAR Shoemaker. Eros was first discovered on August 13, 1898 by a German astronomer, Carl Gustav, and named after a god of love and beauty in Greek mythology. It is the second largest near-Earth asteroid orbiting between the orbits of the Earth and Mars. The average distance from the sun is 1.46 astronomical units, which is two hundred and eighteen million kilometers. The orbital parameters of Eros are shown in Table 1.1. The C_{10}, C_{11} terms are zero because the origin of the coordinate frame for this model is at the center of mass of the asteroid. The C_{21} term is equal to zero since the z axis alines with the spin axis. All the parameters were obtained from Jet Propulsion Laboratory data base [8] and from Sheeres' paper [5]. Table 1.2 shows the position of Eros in cartesian coordinates and orbital elements at the epoch February 14, 2000, 16:00:00 ET.

Table 1.1: Properties of 433 Eros [8].

Parameter	Value	Unit
Size	$34.4 \times 11.2 \times 11.2$	km
Gravitational Parameter $\mu = GM$	4.4631×10^{-4}	km^3/s^2
Mass	6.687×10^{15}	kg
Volume	2503	km^3
Characteristic Length	9.933	km
Density	2.67	g/cm^3
Normalized Principal Morment of Inertia J_{xx}	17.09	km^2
Normalized Principal Morment of Inertia J_{yy}	71.79	km^2
Normalized Principal Morment of Inertia J_{zz}	74.49	km^2
Pole Right Ascension	11.369	deg
Rotation Rate	0.000331	rad/sec
Orbital Period	1.76	years
Gravitational Parameter C_{20}	-0.0878	
Gravitational Parameter C_{22}	0.0439	

Table 1.2: Estimates of Eros's heliocentric orbit [5].

Epoch February 14, 2000, 16:00:00 ET		
Element	Value	Unit
Cartesian		
X	-1.372619235×10^8	km
Y	-1.404571499×10^8	km
Z	-1.045890113×10^8	km
$\dot{X}$	$+1.488152028 \times 10^1$	km/s
$\dot{Y}$	-1.759628159×10^1	km/s
$\dot{Z}$	-7.314516907×10^0	km/s
Orbital		
Semi-Major Axis a	2.181658374×10^8	km
Eccentricity e	0.222764914	-
Inclination i	30.805595	deg
Argument of Perigee ω	138.798959	deg
Longitude of the Ascending Node Ω	342.384153	deg
True Anomaly η	107.814684	deg

Figure 1.2: 433 Eros [11].

1.4 Contribution of Thesis

This thesis presents an effective control scheme for a spacecraft orbiting the asteroid 433 Eros and provides a 3-D simulation. The thesis first summarizes the progress made in the dynamics formulation and then provides a framework for the control system design. Using established control techniques, methods are constructed to control both rotational and translational motion of the spacecraft. A new quaternion feedback control law is constructed using Lyapunov's second method. Computer simulations are carried out to illustrate the effectiveness of the control laws.

1.5 Organization of Thesis

The organization of the thesis is as follows: Chapter 2 summarizes the basics of Lyapunov's stability theory. In Chapter 3, we summarize the gravitational potential field model of a nonspherical body. Chapter 4 introduces the translational and rotational dynamics of a spacecraft orbiting an asteroid. Chapter 5 is devoted to translational and rotational control law design. Chapter 6 presents conclusions.

Chapter 2

Background on Lyapunov Stability Theory

2.1 Introduction to Lyapunov's Stability Theory

One of Aleksandr Lyapunov's main contributions to control theory involves his method of determining stability of nonlinear systems. Lyapunov's stability criteria and theorems play an important role in both the translational and rotational control schemes developed in this thesis. In developing these control schemes, Lyapunov's second stability theorem and LaSalle's invariance principle are used to prove that each control law is effective. This chapter briefly describes Lyapunov's stability criteria and summarizes the results on Lyapunov's second stability method. For full details on Lyapunov's stability theory, see [13], [15].

Let $\boldsymbol{x} = (x_1, x_2, \cdots, x_n)^T$ denote an n dimensional state vector and consider an autonomous nonlinear dynamical system written in the form

$$\dot{\boldsymbol{x}} = \boldsymbol{f}(\boldsymbol{x}), \tag{2.1}$$

where the $\boldsymbol{f}(\boldsymbol{x})$ function is considered to be continuously differentiable.
In this thesis an "overdot" represents differentiation with respect to time, i.e. $\dot{\boldsymbol{x}} \triangleq d\boldsymbol{x}/dt$. Let $\boldsymbol{x_e}$ denote an equilibrium state defined as

$$\boldsymbol{f}(\boldsymbol{x_e}) = 0. \tag{2.2}$$

- The equilibrium state $\boldsymbol{x_e}$ is said to be *Lyapunov stable* if for any $\varepsilon > 0$ there exists a real positive number $\delta(\varepsilon, t_0)$ such that

  $$\parallel \boldsymbol{x}(t_0) - \boldsymbol{x_e} \parallel \leq \delta(\varepsilon, t_0) \Rightarrow \parallel \boldsymbol{x}(t) - \boldsymbol{x_e} \parallel \leq \varepsilon, \qquad \text{for all } t \geq t_0$$

  where $\parallel \boldsymbol{x} \parallel$ denotes the Euclidean norm of a vector $\boldsymbol{x}$;

  $$\parallel \boldsymbol{x} \parallel \equiv \sqrt{\boldsymbol{x}^T \boldsymbol{x}}.$$

- The equilibrium state $\boldsymbol{x_e}$ is said to be *locally asymptotically stable* if it is *Lyapunov stable* as explained above and if

  $$\parallel \boldsymbol{x}(t_0) - \boldsymbol{x_e} \parallel \leq \delta(\varepsilon, t_0) \;\Rightarrow\; \boldsymbol{x}(t) \to \boldsymbol{x_e} \qquad \text{as } t \to \infty.$$

- The equilibrium point $\boldsymbol{x_e}$ is said to be *globally asymptotically stable* if both of the above conditions are met for any initial conditions $\boldsymbol{x}(t_0)$.

Essentially, if it can be shown that the control laws presented here provide global asymptotic stability, then starting from any initial condition the system will reach the desired equilibrium state.

Proving the stability of nonlinear systems with the basic stability definitions and

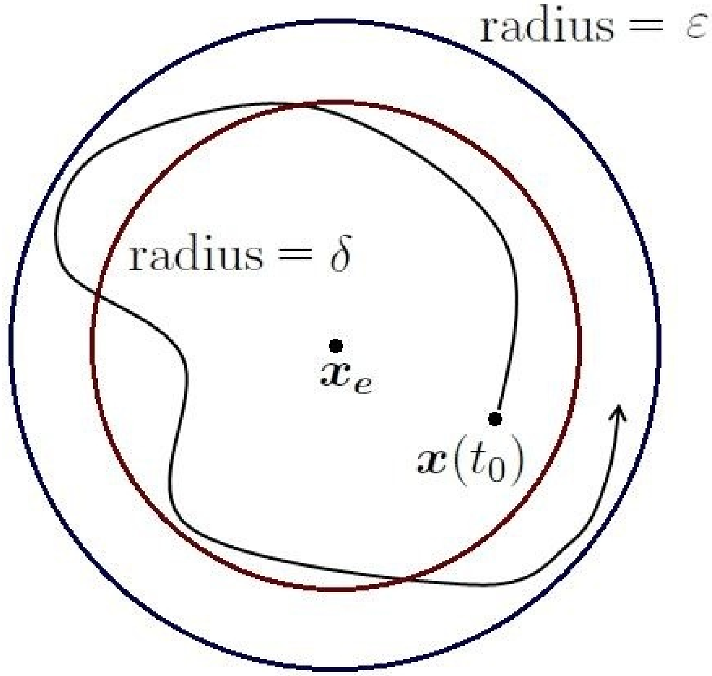

Figure 2.1: Lyapunov Stable.

without resorting to local approximations can be quite tedious and difficult. Lyapunov's direct method provides a tool to make rigorous, analytical stability claims of nonlinear systems by studying the behavior of a scalar, energy-like Lyapunov function.

Let $E(\boldsymbol{x})$ be a continuously differentiable function defined on a domain $D\subset R^n$, which contains the equilibrium state. Then we have the following definitions:

- $E(\boldsymbol{x})$ is said to be positive definite if

$$E(\boldsymbol{x_e}) = 0 \text{ and } E(\boldsymbol{x}) > 0, \text{for all } \boldsymbol{x} \neq \boldsymbol{x_e} \text{ in the domain } D.$$

- $E(x)$ is positive semidefinite in the same domain if

$$E(\boldsymbol{x}) \geq 0, \text{for all } \boldsymbol{x} \text{ in the domain D as t} \rightarrow \infty.$$

Negative definite and negative semidefinite are defined as: if $-E(\boldsymbol{x})$ is negative definite or if $-E(\boldsymbol{x})$ is negative semidefinite, respectively.

2.2 Lyapunov's Second Stability Theorem

Consider the dynamical system (2.1) and assume that $\boldsymbol{x}$ is an isolated equilibrium state. If a positive-definite scalar function $E(\boldsymbol{x})$ exists in a region D around the equilibrium state $\boldsymbol{x_e}$, with continuous first partial derivatives with respect to x_i, see below:

1. $E(\boldsymbol{x}) > 0$ for all $\boldsymbol{x} \neq \boldsymbol{x_e}$ in the domain D, $E(\boldsymbol{x_e})$=0.

2. $\dot{E}(\boldsymbol{x}) \leq 0$ for all $\boldsymbol{x} \neq \boldsymbol{x_e}$ in the domain D.

Then the equilibrium point $\boldsymbol{x_e}$ is *stable*.
In addition to the conditions 1 and 2,

3. the equilibrium point $\boldsymbol{x_e}$ is *locally asymptotically stable*, if $\dot{E}(\boldsymbol{x})$ is not identically zero along any solution of (2.1) other than the equilibrium point $\boldsymbol{x_e}$.

In addition to the condition 3,

4. the equilibrium point is *globally asymptotically stable*, i.e. $\boldsymbol{x}(t) \rightarrow \boldsymbol{x_e}$ as t $\rightarrow\infty$ for any initial condition $\boldsymbol{x}(t_0)$, if there exists in the entire state space a positive-definite function $E(\boldsymbol{x})$ which is radially unbounded, i.e. $E(\boldsymbol{x}) \rightarrow \infty$ as $\| \boldsymbol{x} \| \rightarrow \infty$.

Note that conditions 3 and 4 follow directly from LaSalle's invariance principle.

Chapter 3

Gravitational Potential Field Model

The development in this chapter follows that in [9].

3.1 Gravitational Potential Approximation

3.1.1 Gravitational Potential Field Models

The gravitational potential $\mathrm{d}U$ at a point P (representing the spacecraft position) by the small elements $\mathrm{d}m$ is of the form

$$\mathrm{d}U = G\frac{\mathrm{d}m}{s}, \tag{3.1}$$

where $s = ||\boldsymbol{s}||$ and $\boldsymbol{s}$ is the position vector from the small element $\mathrm{d}m$ to the point P. The position vector $\boldsymbol{s}$ can be expressed as

$$\boldsymbol{s} = \boldsymbol{r} - \boldsymbol{\rho}, \tag{3.2}$$

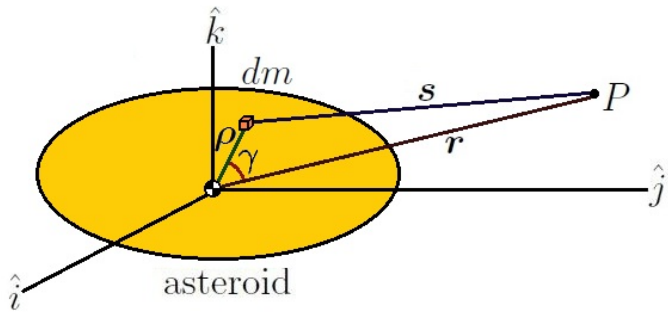

Figure 3.1: Geometry

where $\boldsymbol{\rho}$ is the position vector of the small element $\mathrm{d}m$ from the center of mass of the asteroid and $\boldsymbol{r}$ is the position vector of the point P from the asteroid center of mass as shown in Figure 3.1.

The magnitude of the vector $\boldsymbol{s}$ can be expressed as

$$s = r(1 - 2\nu\alpha + \alpha^2)^{1/2}, \tag{3.3}$$

where $\nu = \cos\gamma$ and $\alpha = \rho/r$ if $\rho/r < 1$ or $\alpha = r/\rho$ if $\rho/r > 1$. γ is the angle between $\boldsymbol{\rho}$ and $\boldsymbol{r}$.

Using the binomial theorem, it can be obtained as

$$(1 - 2\nu\alpha + \alpha^2)^{-\frac{1}{2}} = \sum_{k=0}^{\infty} P_k(\nu)\alpha^k, \tag{3.4}$$

for $\alpha < 1$, where $P_k(\nu)$ denotes the Legendre polynomials, which are obtained as

$$P_0(\nu) = 1, \tag{3.5}$$

$$P_1(\nu) = \nu, \tag{3.6}$$

$$P_{n+1}(\nu) = \frac{2n+1}{n+1}\nu P_n(\nu) - \frac{n}{n+1}P_{n-1}(\nu). \tag{3.7}$$

Thus the gravitational potential of the small element dm can be rewritten as

$$\mathrm{d}U = G\frac{\mathrm{d}m}{r}\sum_{k=0}^{\infty}\left(\frac{\rho}{r}\right)^k P_k(\cos\gamma). \tag{3.8}$$

Therefore the gravitational potential field of the asteroid be expressed as

$$U(r) = G\frac{m}{r} + \frac{G}{r}\sum_{k=1}^{\infty}\iiint\left(\frac{\rho}{r}\right)^k P_k(\cos\gamma)\,\mathrm{d}m. \tag{3.9}$$

3.1.2 MacCullagh's Approximation

If the distance between the point P and the center of mass is large compared with the dimensions of the body, the gravitational potential can be approximated as

$$U(r) = G\frac{m}{r} + \frac{G}{r^2}\iiint \rho\cos\gamma\,\mathrm{d}m + \frac{G}{2r^3}\iiint \rho^2(3\cos\gamma^2 - 1)\,\mathrm{d}m. \tag{3.10}$$

If the origin C of the coordinate frame and the center of mass of the body are the same, we can obtain

$$\iiint \rho\cos\gamma\,\mathrm{d}m = 0. \tag{3.11}$$

The moment of inertia about each axis is of the form

$$J_{\xi\xi} = \iiint(\eta^2 + \zeta^2)\,\mathrm{d}m, \tag{3.12}$$

$$J_{\eta\eta} = \iiint(\xi^2 + \zeta^2)\,\mathrm{d}m, \tag{3.13}$$

$$J_{\zeta\zeta} = \iiint(\eta^2 + \xi^2)\,\mathrm{d}m, \tag{3.14}$$

$$J_{\xi\xi} + J_{\eta\eta} + J_{\zeta\zeta} = 2\iiint \rho^2\,\mathrm{d}m = 0, \tag{3.15}$$

where ξ, η, and ζ are the coordinates of dm in the asteroid body fixed frame of reference.

Defining the moment of inertia of the body about the line connecting the center of mass and the point P, we obtain

$$J_r = \iiint \rho^2 \sin^2 \gamma \, \mathrm{d}m. \tag{3.16}$$

Therefore the potential (3.10) can be expressed in terms of moments of inertia as

$$U(r) = G\frac{m}{r} + \frac{G}{2r^3}(J_{\xi\xi} + J_{\eta\eta} + J_{\zeta\zeta} - 3J_r). \tag{3.17}$$

3.1.3 Spherical Harmonic Gravitational Potential

In the spherical coordinate system, the position vectors of $\mathrm{d}m$ and the point P, respectively, are

$$\boldsymbol{\rho} = \boldsymbol{\rho}(\rho, \theta, \phi), \tag{3.18}$$

$$\boldsymbol{r} = \boldsymbol{r}(r, \lambda, \delta). \tag{3.19}$$

The small element $\mathrm{d}m$ can be expressed as

$$\mathrm{d}m = D(\rho, \theta, \phi)\rho^2 \cos\beta \, \mathrm{d}\rho \, \mathrm{d}\phi \, \mathrm{d}\theta, \tag{3.20}$$

where $D(\rho, \theta, \phi)$ is the local density of the body.
Using the spherical trigonometry, $\cos\gamma$ can be expressed as

$$\cos\gamma = \sin\delta \sin\phi + \cos\delta \cos\phi \cos(\lambda - \theta). \tag{3.21}$$

The associated Legendre function is

$$P_k^j(\nu) = (1 - \nu^2)^{j/2} \frac{\mathrm{d}^j}{\mathrm{d}\nu^j} P_k(\nu), \tag{3.22}$$

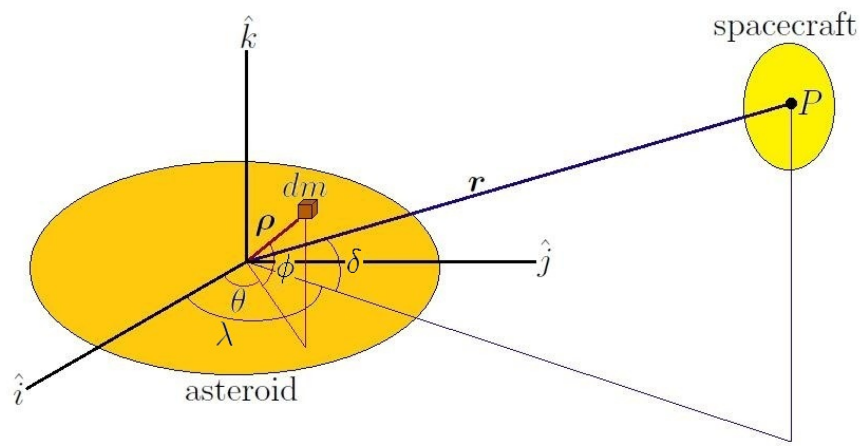

Figure 3.2: Position vectors in spherical coordinates.

where the parameters j and k are referred to as the order and degree, respectively. Zeroth-order Legendre function is defined as

$$P_k^0(\nu) = P_k(\nu), \tag{3.23}$$

$$P_k^j(\nu) = 0,\ \forall j > k. \tag{3.24}$$

Equation (3.21) can be rewritten in terms of the associated Legendre functions as

$$P_1(\cos\gamma) = P_1(\sin\delta)P_1(\sin\phi) + P_1^1(\sin\delta)P_1^1(\sin\phi)\cos(\lambda-\theta). \tag{3.25}$$

Therefore the zeroth-order kth-degree Legendre function of $\cos\gamma$ can be written as

$$P_k(\cos\gamma) = P_k(\sin\delta)P_k(\sin\phi) + 2\sum_{j=1}^{k}\frac{(k-j)!}{(k+j)!}P_k^j(\sin\delta)P_k^j(\sin\phi)\cos j(\lambda-\theta). \tag{3.26}$$

Hence the gravitational potential can be written as

$$U(r) = \frac{Gm}{r} + \sum_{k=1}^{\infty} \frac{1}{r^{k+1}} \left[\overline{C}_{k0} P_k(\sin\delta) + \sum_{j=1}^{k} P_k^j(\sin\delta) \left(\overline{C}_{kj} \cos j\lambda + \overline{S}_{kj} \sin j\lambda \right) \right], \tag{3.27}$$

where

$$\overline{C}_{k0} = G \iiint \rho^{k+2} D(\rho, \theta, \phi) P_k(\sin\theta) \cos\theta \, \mathrm{d}\rho \, \mathrm{d}\theta \, \mathrm{d}\phi, \tag{3.28}$$

$$\overline{C}_{kj} = 2G \frac{(k-j)!}{(k+j)!} \iiint \rho^{k+2} D(\rho, \theta, \phi) P_k^j(\sin\theta) \cos(j\phi) \cos\theta \, \mathrm{d}\rho \, \mathrm{d}\theta \, \mathrm{d}\phi, \tag{3.29}$$

$$\overline{S}_{kj} = 2G \frac{(k-j)!}{(k+j)!} \iiint \rho^{k+2} D(\rho, \theta, \phi) P_k^j(\sin\theta) \sin(j\phi) \cos\theta \, \mathrm{d}\rho \, \mathrm{d}\theta \, \mathrm{d}\phi. \tag{3.30}$$

The standard gravity field would be used for navigation operations about a small body can be estimated from the radiometric data, combined with optimal data. The usual specification of this field is truncated at some degree and order and is expressed as

$$U(r) = \frac{Gm}{r} \sum_{i=0}^{N} \sum_{j=0}^{i} \left(\frac{r_0}{r} \right)^i P_i^j(\sin\delta) [C_{ij} \cos j\lambda + S_{ij} \sin j\lambda], \tag{3.31}$$

where r_0 is the characteristic length of the small body and

$$C_{i0} = \frac{\overline{C}_{i0}}{Gmr_0^i}, \qquad C_{ij} = \frac{\overline{C}_{ij}}{Gmr_0^i} \ (\text{for } j \neq 0), \qquad S_{ij} = \frac{\overline{S}_{kj}}{Gmr_0^i} \tag{3.32}$$

For many practical applications, the assumption of axial symmetry for a body is reasonable. The gravitational potential of such bodies is given by

$$U(r) = \frac{Gm}{r} \left[1 - \sum_{k=2}^{\infty} \left(\frac{r_0}{r} \right)^k J_k P_k(\sin\delta) \right], \tag{3.33}$$

where J_k is the kth zonal harmonics.

The perturbing function is given by

$$R = -\frac{Gm}{r} \sum \left(\frac{r_0}{r}\right)^k J_k P_k(\sin\delta). \tag{3.34}$$

Thus the perturbing acceleration can be written in spherical coordinates as

$$f = \nabla R = \frac{\partial R}{\partial r}\hat{i}_r + \frac{1}{r}\frac{\partial R}{\partial \phi}\hat{i}_\phi + \frac{1}{r\cos\phi}\frac{\partial R}{\partial \theta}\hat{i}_\theta. \tag{3.35}$$

3.2 Gravity-Gradient Torque

In this section, we made the following assumptions in deriving the equations of motion following the development in [9]:

- The spacecraft is rigid.
- The external force acting on the spacecraft is only the gravitational attraction of the asteroid.
- The rotation rate of the asteroid $\mathbf{\Omega}$ is constant and rotating about the vector $\hat{K}$.
- The orbital motion of the spacecraft is described as a closed, planar, and periodic orbit.
- The orbital motion of the spacecraft is not affected by attitude dynamics.

Thus the attitude motion can be described by Euler's equation of motion of a rigid body.

$$J_1\dot{\omega}_1 - (J_2 - J_3)\,\omega_2\omega_3 = M_1, \tag{3.36a}$$

$$J_2\dot{\omega}_2 - (J_3 - J_1)\,\omega_3\omega_1 = M_2, \tag{3.36b}$$

$$J_3\dot{\omega}_3 - (J_1 - J_2)\,\omega_1\omega_2 = M_3, \tag{3.36c}$$

where J_i is the principal moments of inertia of spacecraft, ω_i is the angular velocity along the principal axes, and M_i is the external moment about the principal axes.

3.2.1 Coordinate Systems

- A set of three orthogonal unit vectors $(\hat{I}, \hat{J}, \hat{K})$ defines the inertial frame $\mathcal{F}_i$.
- A set of three orthogonal unit vectors $(\hat{\imath}, \hat{\jmath}, \hat{k})$ defines the asteroid body fixed frame $\mathcal{F}_a$. The vectors are aligned with the three centroidal principal axes of the smallest, intermediate, and largest moments of inertia of the asteroid. The vector $\hat{k}$ points in the same direction as $\hat{K}$ in this thesis.
- A set of three orthogonal unit vectors $(\hat{o}_1, \hat{o}_2, \hat{o}_3)$ defines the orbital frame $\mathcal{F}_o$. The origin of this frame is at the center of mass of the spacecraft. $\hat{o}_3$ points towards the center of mass of the asteroid, $\hat{o}_1$ points towards the transverse direction in the orbital plane, and $\hat{o}_2 = \hat{o}_3 \times \hat{o}_1$.
- A set of three orthogonal unit vectors $(\hat{b}_1, \hat{b}_2, \hat{b}_3)$ defines the spacecraft body fixed frame $\mathcal{F}_b$ and defined along the principal axes of the spacecraft.
- A set of three orthogonal unit vectors $(\hat{e}_R, \hat{e}_\lambda, \hat{e}_\delta)$ are associated with the spherical coordinate system (R, λ, δ) as shown in Figure 3.4. Here λ and δ denote the longitude and latitude of $\mathrm{d}m$, respectively.

$\boldsymbol{R}_c$ is the position vector of the center of mass of the spacecraft (CM_s) from the center of mass of the asteroid (CM_a). In the orbital frame $\mathcal{F}_o$:

$$\boldsymbol{R}_c = -R_c\,\hat{o}_3. \tag{3.37}$$

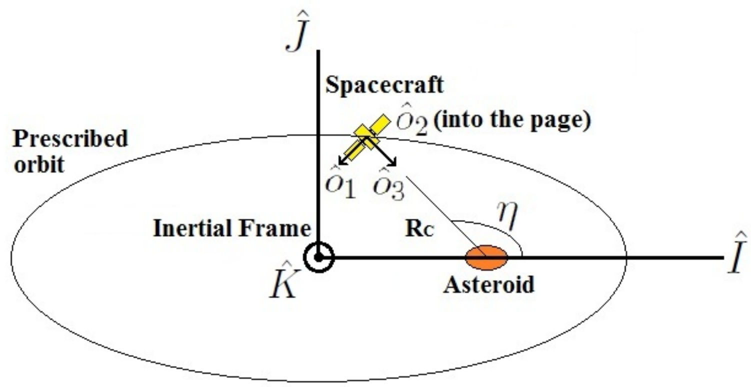

Figure 3.3: Inertial frame and orbital frame in equatorial plane

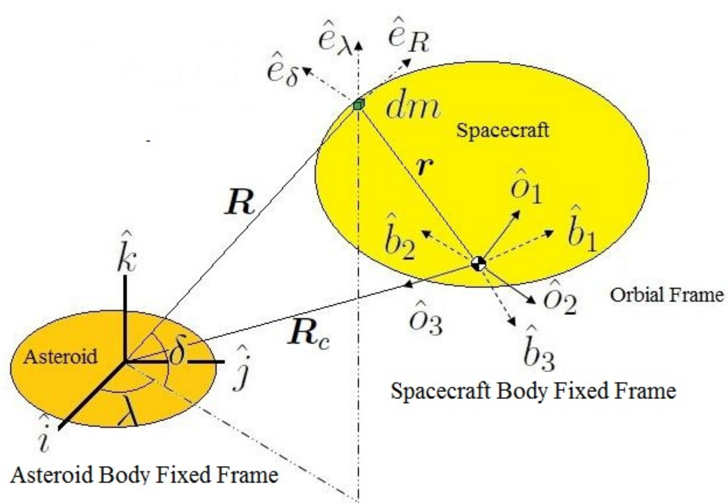

Figure 3.4: Spacecraft body fixed frame, orbital frame, and asteroid body fixed frame.

Let $\boldsymbol{r}$ denote the position vector of dm in CM_s. In the spacecraft body fixed frame $\mathcal{F}_b$:

$$\boldsymbol{r} = x\,\hat{b}_1 + y\,\hat{b}_2 + z\,\hat{b}_3. \tag{3.38}$$

Denote by $\boldsymbol{R}$ the position vector of dm in CM_a. In terms of $\boldsymbol{r}$ and $\boldsymbol{R}_c$,

$$\boldsymbol{R} = \boldsymbol{R}_c + \boldsymbol{r}. \tag{3.39}$$

Throughout this thesis, we assume that $\boldsymbol{R}$ and $\boldsymbol{R}_c$ is much greater than $\boldsymbol{r}$.

The $C_1(\theta_1) \leftarrow C_2(\theta_2) \leftarrow C_3(\theta_3)$ rotation sequence is used to obtain the rotation matrix from the orbital frame $\mathcal{F}_o$ to the spacecraft body fixed frame $\mathcal{F}_b$:

$$\mathcal{F}_b = C_1(\theta_1)C_2(\theta_2)C_3(\theta_3)\mathcal{F}_o = C\mathcal{F}_o, \tag{3.40}$$

where C is the direction cosine matrix and C_i is the rotation matrix of each rotation

$$C_1(\theta_1) = \begin{bmatrix} 1 & 0 & 0 \\ 0 & \cos\theta_1 & \sin\theta_1 \\ 0 & -\sin\theta_1 & \cos\theta_1 \end{bmatrix}, \tag{3.41a}$$

$$C_2(\theta_2) = \begin{bmatrix} \cos\theta_2 & 0 & -\sin\theta_2 \\ 0 & 1 & 0 \\ \sin\theta_2 & 0 & \cos\theta_2 \end{bmatrix}, \tag{3.41b}$$

$$C_3(\theta_3) = \begin{bmatrix} \cos\theta_3 & \sin\theta_3 & 0 \\ -\sin\theta_3 & \cos\theta_3 & 0 \\ 0 & 0 & 1 \end{bmatrix}. \tag{3.41c}$$

Thus the direction cosine matrix C can be obtained as

$$\begin{bmatrix} \hat{b}_1 \\ \hat{b}_2 \\ \hat{b}_3 \end{bmatrix} = C \begin{bmatrix} \hat{o}_1 \\ \hat{o}_2 \\ \hat{o}_3 \end{bmatrix} = \begin{bmatrix} c_2 c_3 & c_2 s_3 & -s_2 \\ s_1 s_2 c_3 - c_1 s_3 & s_1 s_2 s_3 + c_1 c_3 & s_1 c_2 \\ c_1 s_2 s_3 + s_1 s_3 & c_1 s_2 s_3 - s_1 c_3 & c_1 c_2 \end{bmatrix} \begin{bmatrix} \hat{o}_1 \\ \hat{o}_2 \\ \hat{o}_3 \end{bmatrix}, \tag{3.42}$$

where $c_i \triangleq \cos\theta_i$ and $s_i \triangleq \sin\theta_i$.

The angular velocity vector $\boldsymbol{\omega}$ of the spacecraft is represented in the spacecraft body fixed frame $\mathcal{F}_b$ as

$$\boldsymbol{\omega} = \omega_1 \hat{b}_1 + \omega_2 \hat{b}_2 + \omega_3 \hat{b}_3 = \begin{bmatrix} \hat{b}_1 & \hat{b}_2 & \hat{b}_3 \end{bmatrix} \begin{bmatrix} \omega_1 \\ \omega_2 \\ \omega_3 \end{bmatrix}. \tag{3.43}$$

The angular velocity can be obtained as

$$\begin{bmatrix} \omega_1 \\ \omega_2 \\ \omega_3 \end{bmatrix} = \begin{bmatrix} \dot{\theta}_1 \\ 0 \\ 0 \end{bmatrix} + C_1(\theta_1) \begin{bmatrix} 0 \\ \dot{\theta}_2 \\ 0 \end{bmatrix} + C_1(\theta_1) C_2(\theta_2) \begin{bmatrix} 0 \\ 0 \\ \dot{\theta}_3 \end{bmatrix} - \dot{\eta}\hat{K}, \tag{3.44}$$

where $\dot{\eta}$ is the instantaneous orbital rate in the $\hat{K}$-direction.
For the equatorial motion, the vector $\hat{K}$ can be expressed in the spacecraft body fixed frame as

$$\hat{K} = -\hat{o}_2 = -\left(c_2 s_3 \hat{b}_1 + (s_1 s_2 s_3 + c_1 c_3) \hat{b}_2 + (c_1 s_2 s_3 - s_1 c_3) \hat{b}_3 \right). \tag{3.45}$$

Therefore the angular velocity can be written as

$$\begin{bmatrix} \omega_1 \\ \omega_2 \\ \omega_3 \end{bmatrix} = \begin{bmatrix} 1 & 0 & -s_2 \\ 0 & c_1 & s_1 c_2 \\ 0 & -s_1 & c_1 c_2 \end{bmatrix} \begin{bmatrix} \dot{\theta}_1 \\ \dot{\theta}_2 \\ \dot{\theta}_3 \end{bmatrix} - \dot{\eta} \begin{bmatrix} c_2 s_3 \\ s_1 s_2 s_3 + c_1 c_3 \\ c_1 s_2 s_3 - s_1 c_3 \end{bmatrix}. \tag{3.46}$$

3.2.2 Gravitational Force

The gravitational potential (3.31) of an asteroid can be arranged as

$$\begin{aligned} U = \frac{\mu}{R}[1 + \frac{1}{2}\left(\frac{r_0}{R}\right)^2 C_{20}(3\sin^2\delta - 1) + 3\left(\frac{r_0}{R}\right)^2 C_{22}\cos^2\delta\cos(2\lambda) \\ + \frac{1}{2}\left(\frac{r_0}{R}\right)^3 C_{30}\sin\delta(5\sin^2\delta - 3) + \cdots], \end{aligned} \tag{3.47}$$

Keeping only the most significant gravitational coefficients (C_{20} and C_{22}) in the harmonic expansion, the gravitational potential can be arranged as

$$U = \frac{\mu}{R}\left[1 + \frac{1}{2}\left(\frac{r_0}{R}\right)^2 C_{20}(3\sin^2\delta - 1) + 3\left(\frac{r_0}{R}\right)^2 C_{22}\cos^2\delta\cos(2\lambda)\right], \tag{3.48}$$

where r_0 is the characteristic length of the asteroid, R is the distance of the orbiting particle from CM_a, and μ is the gravitational parameter of the asteroid and $\mu = GM$.

The gravitational force acting on dm at a distance R from CM_a can be obtained by taking the partial derivative of the gravitational potential as

$$\begin{aligned} d\boldsymbol{F} &= \left[\frac{\partial U}{\partial R}\hat{e}_R + \frac{1}{R\cos\delta}\frac{\partial U}{\partial\lambda}\hat{e}_\lambda + \frac{1}{R}\frac{\partial U}{\partial\delta}\hat{e}_\delta\right]\mathrm{d}m \\ &= d\boldsymbol{F}_R + d\boldsymbol{F}_\lambda + d\boldsymbol{F}_\delta, \end{aligned} \tag{3.49}$$

where

$$d\boldsymbol{F}_R = -\frac{\mu \mathrm{d}m\boldsymbol{R}}{|\boldsymbol{R}|^3}\left[1+\frac{3}{2}\left(\frac{r_0}{R}\right)^2 C_{20}(3\sin^2\delta-1)+9\left(\frac{r_0}{R}\right)^2 C_{22}\cos^2\delta\cos(2\lambda)\right], \tag{3.50}$$

$$d\boldsymbol{F}_\lambda = -\frac{\mu \mathrm{d}m[\hat{e}_\delta\times\boldsymbol{R}]}{|\boldsymbol{R}|^3}\left[6\left(\frac{r_0}{R}\right)^2 C_{22}\cos\delta\sin\lambda\right], \tag{3.51}$$

$$d\boldsymbol{F}_\delta = -\frac{\mu \mathrm{d}m\hat{e}_\delta}{|\boldsymbol{R}|^2}\left[3\left(\frac{r_0}{R}\right)^2 C_{20}\sin\delta\cos\delta-6\left(\frac{r_0}{R}\right)^2 C_{22}\sin\delta\cos\delta\cos(2\lambda)\right]. \tag{3.52}$$

In the equatorial plane, the latitude δ is negligibly small because $r \ll R, R_c$. Thus the gravitational force for equatorial orbits can be simplified as

$$d\boldsymbol{F}_R = -\frac{\mu \mathrm{d}m\boldsymbol{R}}{|\boldsymbol{R}|^3}\left[1-\frac{3}{2}\left(\frac{r_0}{R}\right)^2 C_{20}+9\left(\frac{r_0}{R}\right)^2 C_{22}\cos 2\lambda\right], \tag{3.53}$$

$$d\boldsymbol{F}_\lambda = -\frac{\mu \mathrm{d}m[\hat{e}_\delta\times\boldsymbol{R}]}{|\boldsymbol{R}|^3}\left[6\left(\frac{r_0}{R}\right)^2 C_{22}\sin\lambda\right], \tag{3.54}$$

$$d\boldsymbol{F}_\delta = 0. \tag{3.55}$$

3.2.3 Gravity-Gradient Torque

The gravity-gradient torque on the spacecraft can be obtained as

$$M = \int \boldsymbol{r}\times d\boldsymbol{F} = \int \boldsymbol{r}\times d\boldsymbol{F}_R + \int \boldsymbol{r}\times d\boldsymbol{F}_\delta + \int \boldsymbol{r}\times d\boldsymbol{F}_\lambda. \tag{3.56}$$

By using the Binomial expansion, each component of the gravity-gradient torque in the spacecraft body fixed frame $\mathcal{F}_b$ can be obtained as

$$\begin{aligned} M_1 =& \frac{\mu}{R^3}[(3+5\phi)(J_3-J_2)c_1c_2^2s_1 + 5\chi(\frac{2}{5}J_1c_2s_3 \\ & -(J_1-J_2+J_3)(c_1c_2c_3s_1s_2+c_2s_1^2s_3) \\ & +(J_2-J_3+J_1)(c_1c_2c_3s_1s_2-c_1^2c_2s_3))], \end{aligned} \tag{3.57}$$

$$\begin{aligned} M_2 =& \frac{\mu}{R^3}[(3+5\phi)(J_3-J_1)c_1c_2s_2 + \frac{5}{2}\chi(\frac{2}{5}J_2(s_1s_2s_3+c_1c_3) \\ & -(J_2-J_1+J_3)(c_1c_3s_2^2+s_1s_2s_3)-(J_2-J_3+J_1)c_1c_2^2c_3)], \end{aligned} \tag{3.58}$$

$$\begin{aligned} M_3 =& \frac{\mu}{R^3}[(3+5\phi)(J_1-J_2)c_2s_1s_2 + \frac{5}{2}\chi(\frac{2}{5}J_3(c_1s_2s_3-s_1c_3) \\ & -(J_2-J_1+J_3)(c_1s_2s_3-c_3s_1s_2^2)+(J_1-J_2+J_3)c_2^2c_3s_1)], \end{aligned} \tag{3.59}$$

where

$$\begin{aligned} \phi &= \left(-\frac{3}{2}C_{20}+9C_{22}\cos 2\lambda\right)\left(\frac{r_0}{R}\right)^2, \\ \chi &= 6C_{22}\sin 2\lambda\left(\frac{r_0}{R}\right)^2. \end{aligned}$$

Chapter 4

Translational and Rotational Dynamics

4.1 Translational Dynamics

4.1.1 Equations of Motion

In this section, we describe the translational dynamics of an asteroid orbiting spacecraft shown in Figure 4.1. The development here follows that in [15]. Let $[X, Y, Z]$ and $[x, y, z]$ frames denote an inertial frame $\mathcal{F}_i$ and an asteroid body fixed frame $\mathcal{F}_a$ rotating with the angular velocity $\mathbf{\Omega} = \Omega\hat{\mathbf{K}}$, respectively. Let $\boldsymbol{F}$ denote the translational control force for the spacecraft. Then, the dynamic equations for the translational motion of the spacecraft in the asteroid body fixed frame $\mathcal{F}_a$ are given by

$$m\ddot{\boldsymbol{R}} = m\nabla U + \boldsymbol{F}, \tag{4.1}$$

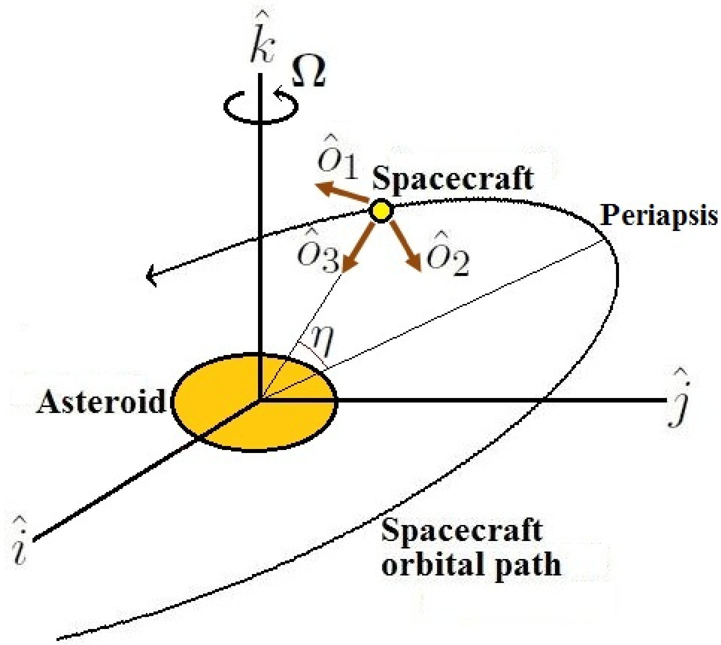

Figure 4.1: Translational motion.

where R is the inertial position of the spacecraft in the asteroid frame, m is the spacecraft mass, and U is the gravitational potential given as

$$U = \frac{\mu}{R}\left[1 + \frac{1}{2}\left(\frac{r_0}{R}\right)^2 C_{20}(3\sin^2\delta - 1) + 3\left(\frac{r_0}{R}\right)^2 C_{22}\cos^2\delta\cos(2\lambda)\right]. \tag{4.2}$$

The $\sin\delta$, $\cos\delta$, and R terms can be expressed in terms of x, y, and z as

$$\sin^2\delta = \frac{z^2}{R^2}, \tag{4.3}$$

$$\cos^2\delta = \frac{x^2+y^2}{R^2}, \tag{4.4}$$

$$R^2 = x^2 + y^2 + z^2. \tag{4.5}$$

Thus, equation (4.2) can be expressed as

$$U = \mu \left[R^{-1} + \frac{3}{2} r_0^2 C_{20} z^2 R^{-5} - \frac{1}{2} r_0^2 C_{20} R^{-3} + 3 r_0^2 C_{22} \cos(2\lambda)(x^2 + y^2) R^{-5} \right]. \quad (4.6)$$

The translational dynamics of the spacecraft in the asteroid body fixed frame $\mathcal{F}_a$ can be rewritten as

$$m\ddot{\boldsymbol{R}} = m \left(\frac{\partial U}{\partial x} \hat{i} + \frac{\partial U}{\partial y} \hat{j} + \frac{\partial U}{\partial z} \hat{k} \right) + \boldsymbol{F}, \quad (4.7)$$

where

$$\begin{aligned} \frac{\partial U}{\partial x} =& - \mu x R^{-3} [1 + \frac{15}{2} r_0^2 C_{20} z^2 R^{-4} - \frac{3}{2} r_0^2 C_{20} R^{-2} \\ & - 6 r_0^2 C_{22} \cos(2\lambda) R^{-2} + 15 r_0^2 C_{22} (x^2 + y^2) \cos(2\lambda) R^{-4}], & (4.8) \\ \frac{\partial U}{\partial y} =& - \mu y R^{-3} [1 + \frac{15}{2} r_0^2 C_{20} z^2 R^{-4} - \frac{3}{2} r_0^2 C_{20} R^{-2} \\ & - 6 r_0^2 C_{22} \cos(2\lambda) R^{-2} + 15 r_0^2 C_{22} (x^2 + y^2) \cos(2\lambda) R^{-4}], & (4.9) \\ \frac{\partial U}{\partial z} =& - \mu z R^{-3} [1 - \frac{9}{2} r_0^2 C_{20} R^{-2} + \frac{15}{2} r_0^2 C_{20} z^2 R^{-4} \\ & + 15 r_0^2 C_{22} (x^2 + y^2) \cos(2\lambda) R^{-4}]. & (4.10) \end{aligned}$$

Assuming that Ω is constant, the acceleration of the spacecraft $\ddot{\boldsymbol{R}}$ also can be written as

$$\ddot{\boldsymbol{R}} = \boldsymbol{a} + 2\boldsymbol{\Omega} \times \boldsymbol{v} + \boldsymbol{\Omega} \times (\boldsymbol{\Omega} \times \boldsymbol{R}), \quad (4.11)$$

where

$$\boldsymbol{a} = [\ddot{x},\, \ddot{y},\, \ddot{z}]^T, \quad (4.12)$$

$$\boldsymbol{v} = [\dot{x},\, \dot{y},\, \dot{z}]^T, \quad (4.13)$$

$$\boldsymbol{\Omega} = [0,\, 0,\, \Omega]^T. \quad (4.14)$$

Thus the acceleration can be written as

$$\ddot{\boldsymbol{R}} = \begin{bmatrix} \ddot{x} \\ \ddot{y} \\ \ddot{z} \end{bmatrix} + 2 \begin{bmatrix} -\Omega\dot{y} \\ \Omega\dot{y} \\ 0 \end{bmatrix} + \begin{bmatrix} -\Omega^2 x \\ -\Omega^2 y \\ 0 \end{bmatrix}. \tag{4.15}$$

Using equations (4.1) and (4.11), the equations of motion can be obtained as

$$\ddot{\boldsymbol{R}} = \boldsymbol{a} + 2\boldsymbol{\Omega} \times \boldsymbol{v} + \boldsymbol{\Omega} \times (\boldsymbol{\Omega} \times \boldsymbol{R}) = \nabla U + \boldsymbol{F}/m. \tag{4.16}$$

In components these equations can be written as

$$\begin{aligned}
\ddot{x} - 2\Omega\dot{y} - \Omega^2 x = & -\mu x R^{-3}[1 + \frac{15}{2} r_0^2 C_{20} z^2 R^{-4} - \frac{3}{2} r_0^2 C_{20} R^{-2} \\
& - 6 r_0^2 C_{22} \cos(2\lambda) R^{-2} + 15 r_0^2 C_{22}(x^2 + y^2)\cos(2\lambda) R^{-4}] + F_x/m, && (4.17) \\
\ddot{y} + 2\Omega\dot{x} - \Omega^2 y = & -\mu y R^{-3}[1 + \frac{15}{2} r_0^2 C_{20} z^2 R^{-4} - \frac{3}{2} r_0^2 C_{20} R^{-2} \\
& - 6 r_0^2 C_{22} \cos(2\lambda) R^{-2} + 15 r_0^2 C_{22}(x^2 + y^2)\cos(2\lambda) R^{-4}] + F_y/m, && (4.18) \\
\ddot{z} = & -\mu z R^{-3}[1 - \frac{9}{2} r_0^2 C_{20} R^{-2} + \frac{15}{2} r_0^2 C_{20} z^2 R^{-4} \\
& + 15 r_0^2 C_{22}(x^2 + y^2)\cos(2\lambda) R^{-4}] + F_z/m. && (4.19)
\end{aligned}$$

4.1.2 Matlab Simulation

The translational motion of the spacecraft is simulated using Matlab's ode45 integrator in the asteroid and inertial frames. The initial conditions were taken as

$$[x_0,\ y_0,\ z_0] = [R_c,\ 0,\ 0]\,\text{km}, \tag{4.20}$$

$$[\dot{x_0},\ \dot{y_0},\ \dot{z_0}] = \left[0.0001,\ \sqrt{\frac{\mu}{R_c}} - \Omega R_c,\ 0.0001\right]\text{km/sec}, \tag{4.21}$$

where $\mu = 4.4631 \times 10^{-4}\text{km}^3/\text{s}^2$ and $R_c = 50$ km. For the asteroid 433 EROS, the most significant gravitational parameters are given by $C_{20} = -0.0878, C_{22} = 0.0439$, the asteroid rotation rate is $\Omega = 3.31 \times 10^{-4}$ rad/s, and the characteristic length of the asteroid is $r_0 = 9.933$ km. For a direct orbit, the longitude of the spacecraft is calculated as $\lambda = (\dot{\eta} - \Omega)t$. For an uncontrolled translational motion, the control force $\boldsymbol{F}$ is set to be zero.

Figures 4.2, 4.3, 4.4, 4.5, 4.6, and 4.7 show the uncontrolled translational motions of the spacecraft due to the nonuniform gravitational potential of the asteroid. In the subsequent sections, we will develop effective feedback control laws to achieve a circular equatorial orbit.

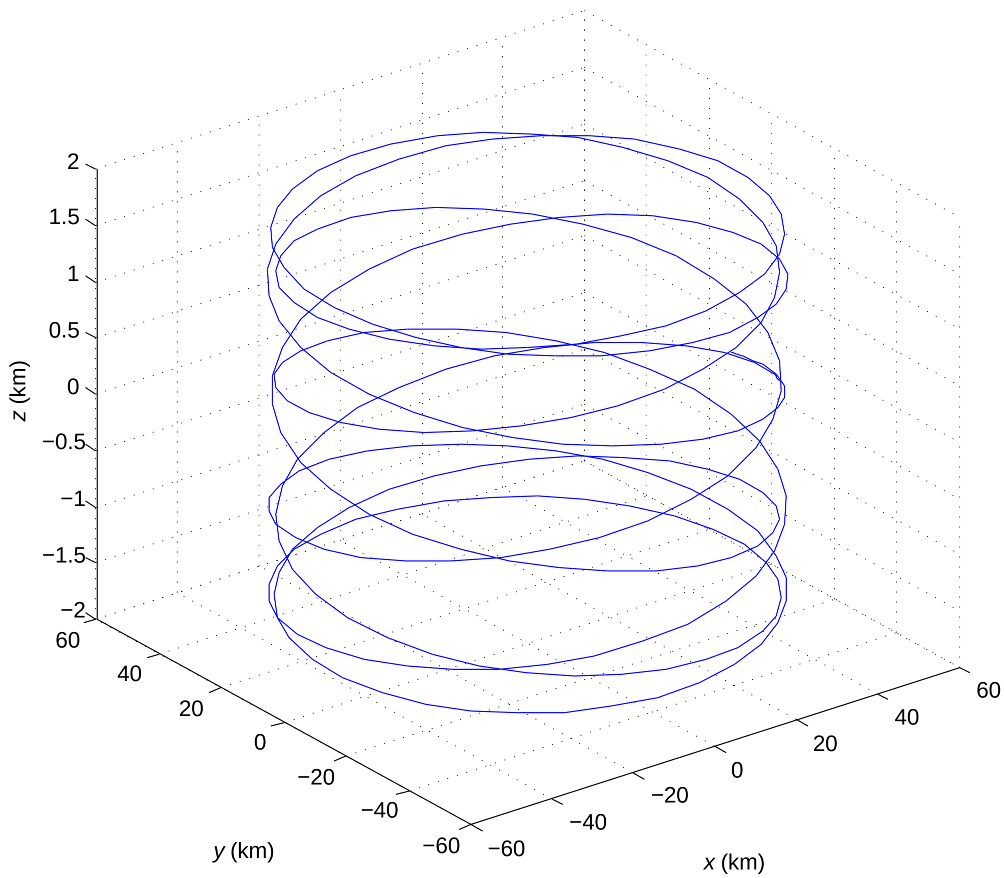

Figure 4.2: Three dimensional uncontrolled spacecraft motion in the the asteroid frame ($R_c = 50$ km).

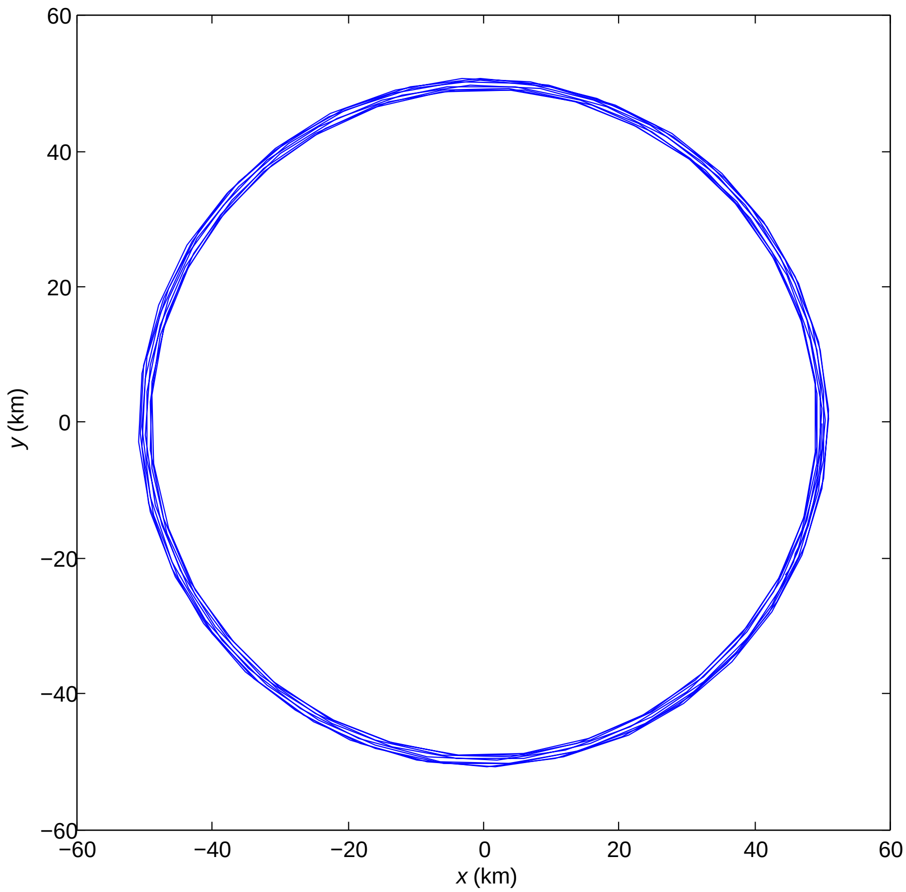

Figure 4.3: Two dimensional uncontrolled spacecraft motion in the asteroid frame ($R_c = 50$ km).

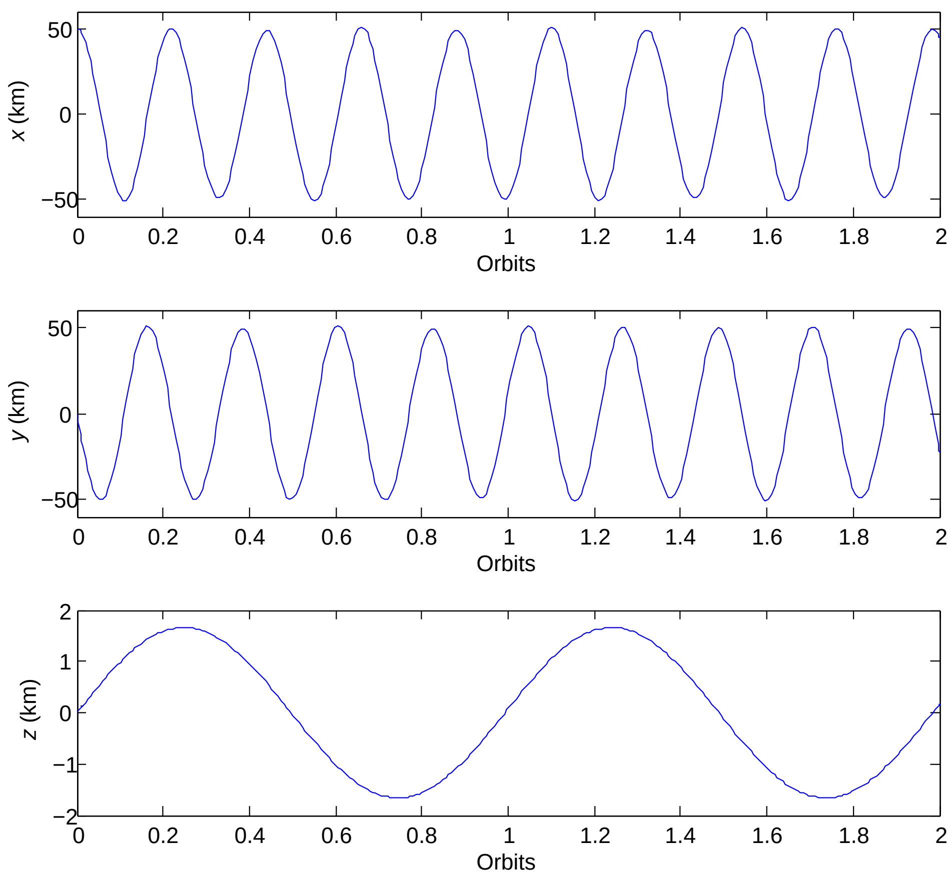

Figure 4.4: Uncontrolled spacecraft x, y, and z positions ($R_c = 50$ km).

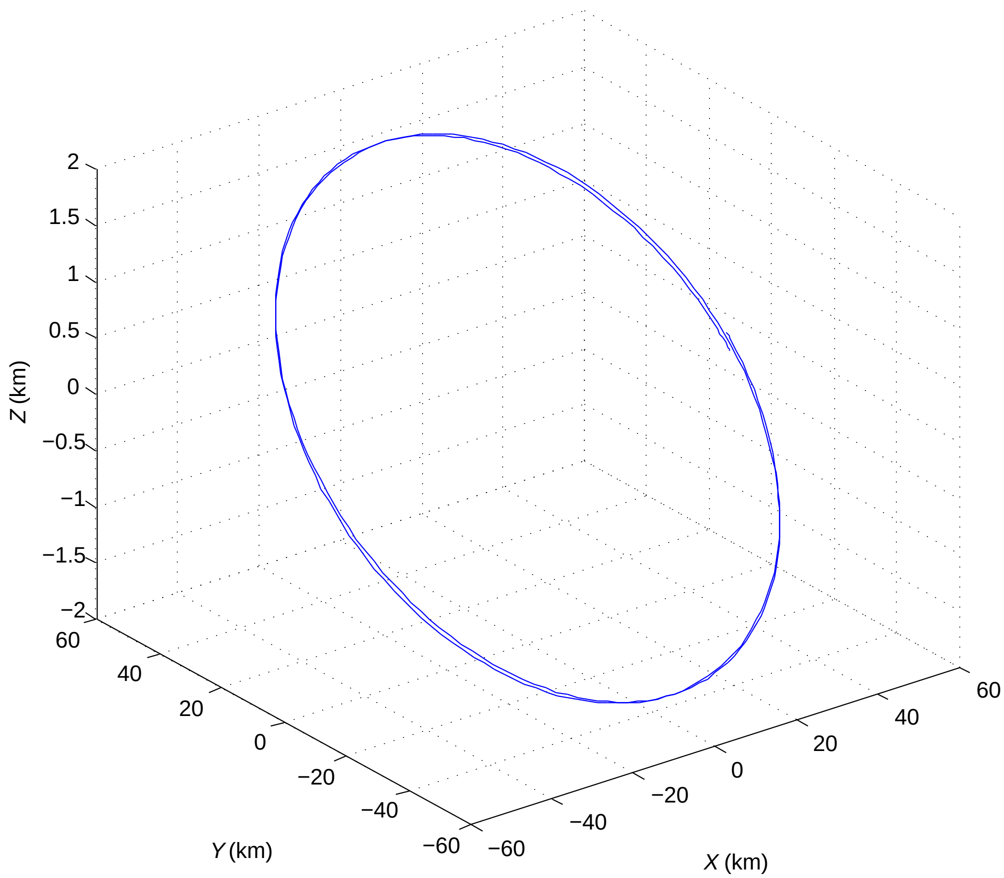

Figure 4.5: Three dimensional uncontrolled spacecraft motion in the the inertial frame ($R_c = 50$ km).

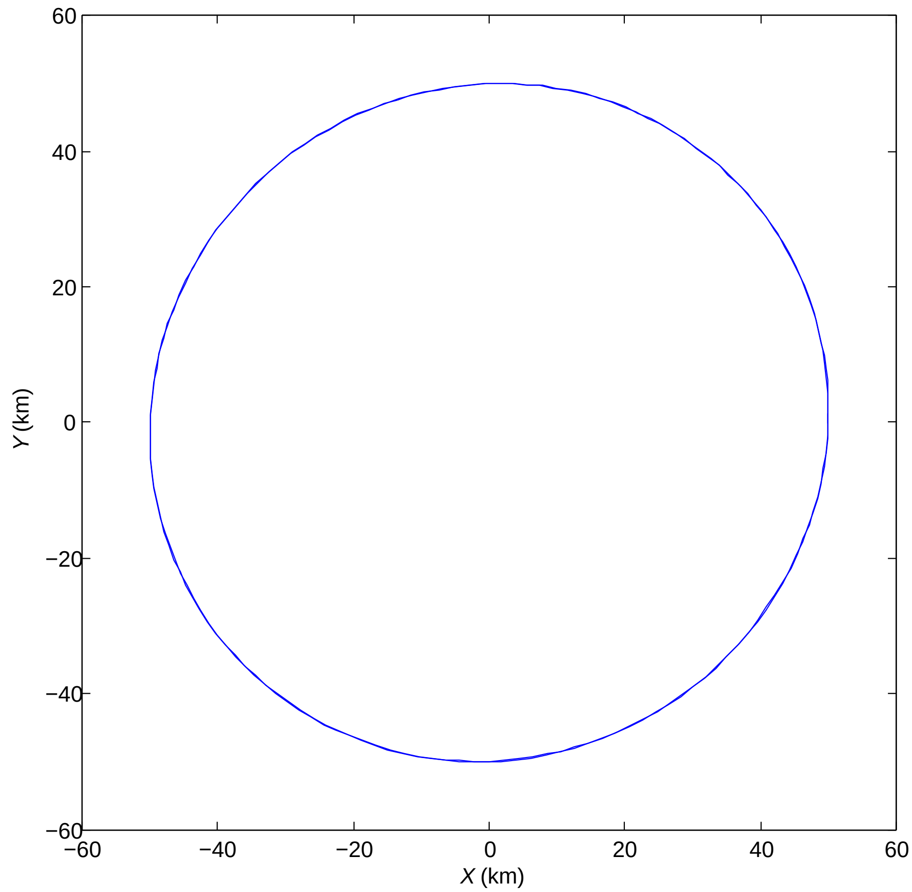

Figure 4.6: Two dimensional uncontrolled spacecraft motion in the inertial frame (R_c = 50 km).

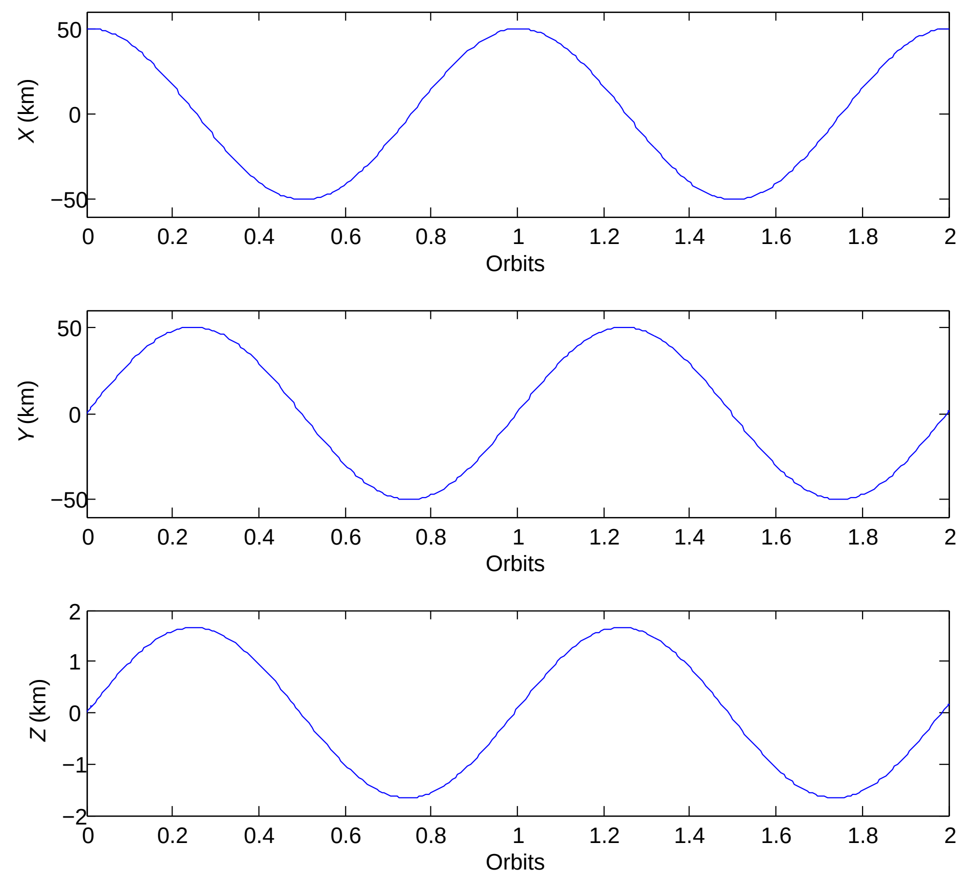

Figure 4.7: Uncontrolled spacecraft X, Y, and Z positions ($R_c = 50$ km).

4.2 Rotational Kinematics and Dynamics

4.2.1 Quaternions

The most commonly used sets of attitude parameters are the Euler angles. They describe the attitude of one frame relative to another. The Euler angles provide a compact, three-parameter attitude description whose coordinates are easy to visualize. One major drawback of these angles is that they result in a geometric singularity. Therefore, their use in describing large rotations is limited. Also, both the rotation matrix and the kinematic equations are highly nonlinear and involve numerous computations of trigonometric functions. Quaternions provide a four-parameter singularity free representation that does not require the calculation of any trigonometric functions. Quaternions, unlike Euler angles, use one axis called an "eigenaxis" to rotate between coordinate systems. In this section, we first briefly review the attitude kinematics and dynamics formulation used in this thesis to obtain the rotational equations of motion for a group of spacecraft. For full details, the reader is referred to [15].

4.2.2 Reference Frames and Rotations

Consider the orbital reference frame $\mathcal{F}_o$, whose three constituent vectors are $\hat{o}_1$, $\hat{o}_2$, and $\hat{o}_3$. Let $\cos\theta_1$, $\cos\theta_2$, and $\cos\theta_3$ be the direction cosines of a vector $\boldsymbol{r}$ as shown in Figure 4.8. Then, we write

$$\boldsymbol{r} = r(\hat{o}_1 \cos\theta_1 + \hat{o}_2 \cos\theta_2 + \hat{o}_3 \cos\theta_3), \tag{4.22}$$

where r is the length of $\boldsymbol{r}$. Now consider the spacecraft body fixed frame $\mathcal{F}_b$, with constituent vectors $\hat{b}_1$, $\hat{b}_2$, and $\hat{b}_3$. A relation between the two reference frames $\mathcal{F}_a$

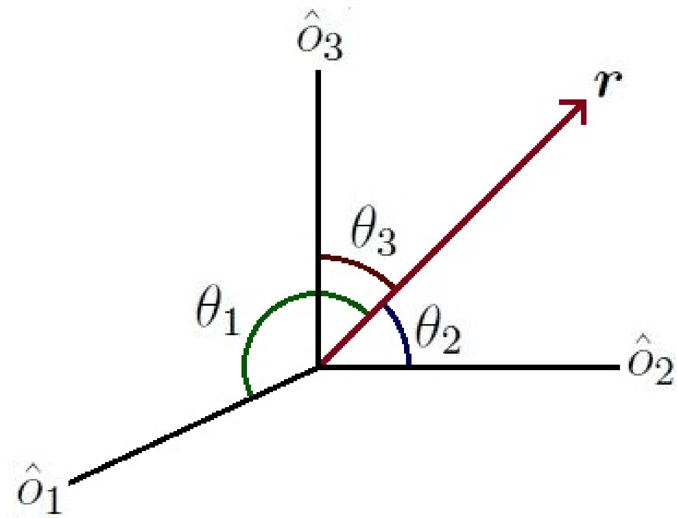

Figure 4.8: Direction cosines between a vector $\boldsymbol{r}$ and the frame $\mathcal{F}_o$.

and $\mathcal{F}_b$ can be written as:

$$\begin{bmatrix} \hat{b}_1 \\ \hat{b}_2 \\ \hat{b}_3 \end{bmatrix} = \begin{bmatrix} c_{11} & c_{12} & c_{13} \\ c_{21} & c_{22} & c_{23} \\ c_{31} & c_{32} & c_{33} \end{bmatrix} \begin{bmatrix} \hat{o}_1 \\ \hat{o}_2 \\ \hat{o}_3 \end{bmatrix}, \tag{4.23}$$

where c_{ij} is the direction cosine between $\hat{b}_i$ and $\hat{o}_j$.

The matrix

$$\boldsymbol{C} = \begin{bmatrix} c_{11} & c_{12} & c_{13} \\ c_{21} & c_{22} & c_{23} \\ c_{31} & c_{32} & c_{33} \end{bmatrix} \tag{4.24}$$

is an orthonormal rotation matrix with the following properties:

$$\boldsymbol{C}\boldsymbol{C}^T = \boldsymbol{C}^T\boldsymbol{C} = \boldsymbol{I}, \qquad \det(\boldsymbol{C}) = +1. \tag{4.25}$$

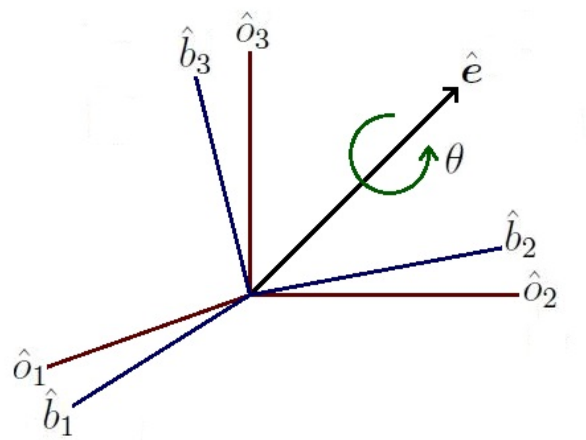

Figure 4.9: Geometry describing Euler's theorem.

where $\boldsymbol{I}$ is the 3×3 identity matrix. The rotation matrix $\boldsymbol{C}$ relates components of a given vector $\boldsymbol{r}$ in the frames $\boldsymbol{F}_a$ and $\boldsymbol{F}_b$ as $\boldsymbol{r}_b = \boldsymbol{C}\boldsymbol{r}_a$.

4.2.3 Rotational Kinematics

Euler's theorem states that the general rotation of a rigid body with one fixed point is a rotation about an axis through that point. Figure 4.9 illustrates the geometry pertaining to Euler's theorem. Now consider an arbitrary vector $\boldsymbol{r}$ as shown in Figure 4.10. As $\mathcal{F}_o$ rotates about an axis $\boldsymbol{e}$ which is called an eigenaxis, by an angle θ which is called an eigenangle, it will appear to an observer fixed in $\mathcal{F}_o$ that $\boldsymbol{r}$ is rotating about $\boldsymbol{e}$ through an angle $-\theta$; to this observer, the rotation corresponds to $\boldsymbol{r} \to \boldsymbol{r'}$, where

$$\boldsymbol{r'} = (\boldsymbol{e} \cdot \boldsymbol{r})\boldsymbol{e} - \boldsymbol{e} \times (\boldsymbol{e} \times \boldsymbol{r}) \cos\theta - \boldsymbol{e} \times \boldsymbol{r} \sin\theta. \tag{4.26}$$

Note that $\boldsymbol{e}^T\boldsymbol{e}$=1. The components of $\boldsymbol{r'}$ in $\mathcal{F}_b$ can then be written as

$$\boldsymbol{r}_b = \left[\boldsymbol{e}\boldsymbol{e}^T + (\boldsymbol{I} - \boldsymbol{e}\boldsymbol{e}^T) \cos\theta - \boldsymbol{E} \sin\theta\right] \boldsymbol{r}_o. \tag{4.27}$$

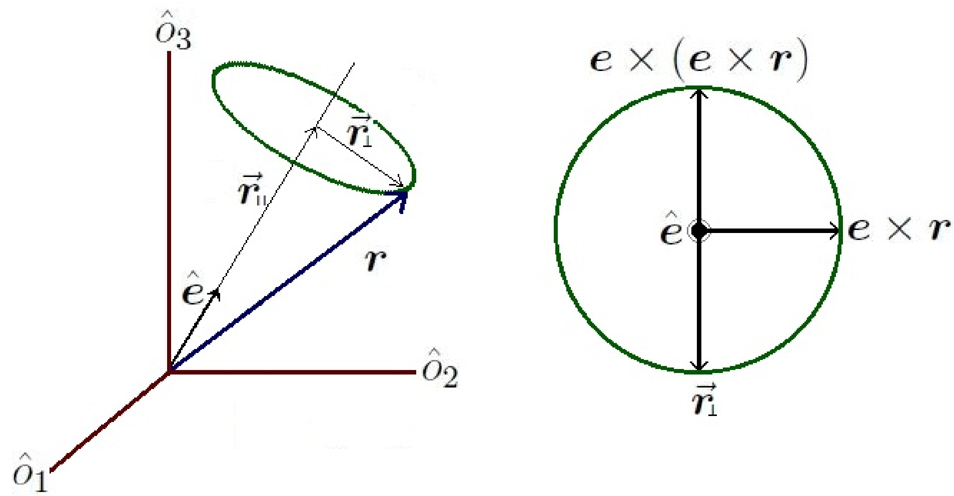

Figure 4.10: Geometrical interpretation of the rotation matrix.

Thus, the rotation matrix can be expressed in terms of $\boldsymbol{e}$ and θ as

$$\boldsymbol{C} = \boldsymbol{e}\boldsymbol{e}^T + \left(\boldsymbol{I} - \boldsymbol{e}\boldsymbol{e}^T\right)\cos\theta - \boldsymbol{E}\sin\theta, \tag{4.28}$$

where $\boldsymbol{E}$ denotes the skew symmetric matrix satisfying $\boldsymbol{e} \times \boldsymbol{r} = \boldsymbol{E}\boldsymbol{r}$, which is given by

$$\boldsymbol{E} = \begin{bmatrix} 0 & -e_3 & e_2 \\ e_3 & 0 & -e_1 \\ -e_2 & e_1 & 0 \end{bmatrix}. \tag{4.29}$$

In full matrix form, the rotation matrix becomes

$$\boldsymbol{C} = \begin{bmatrix} c\theta + e_1^2(1 - c\theta) & e_1e_2(1 - c\theta) + e_3s\theta & e_1e_3(1 - c\theta) - e_2s\theta \\ e_2e_1(1 - c\theta) - e_3s\theta & c\theta + e_2^2(1 - c\theta) & e_2e_3(1 - c\theta) + e_1s\theta \\ e_3e_2(1 - c\theta) + e_2s\theta & e_3e_2(1 - c\theta) - e_1s\theta & c\theta + e_3^2(1 - c\theta) \end{bmatrix}, \tag{4.30}$$

where $c\theta \triangleq \cos\theta$ and $s\theta \triangleq \sin\theta$.

Now quaternions (also called Euler parameters) can be defined as:

$$q_1 = e_1 \sin(\theta/2), \tag{4.31}$$

$$q_2 = e_2 \sin(\theta/2), \tag{4.32}$$

$$q_3 = e_3 \sin(\theta/2), \tag{4.33}$$

$$q_4 = \cos(\theta/2). \tag{4.34}$$

Using the eigenaxis vector $\boldsymbol{e} = (e_1, e_2, e_3)^T$, we define the vector part of the quaternion $\boldsymbol{q} = (q_1, q_2, q_3)^T$ as

$$\boldsymbol{q} = \boldsymbol{e} \sin(\theta/2). \tag{4.35}$$

Note that the quaternions are constrained by the following relationship:

$$\boldsymbol{q}^T\boldsymbol{q} + q_4^2 = q_1^2 + q_2^2 + q_3^2 + q_4^2 = 1. \tag{4.36}$$

The rotation matrix $\boldsymbol{C}$ can be parameterized in terms of quaternions as

$$\boldsymbol{C} = \begin{bmatrix} 1 - 2\left(q_2^2 + q_3^2\right) & 2\left(q_1q_2 + q_3q_4\right) & 2\left(q_1q_3 - q_2q_4\right) \\ 2\left(q_2q_1 - q_3q_4\right) & 1 - 2\left(q_3^2 + q_1^2\right) & 2\left(q_2q_3 + q_1q_4\right) \\ 2\left(q_3q_1 + q_2q_4\right) & 2\left(q_3q_2 - q_1q_4\right) & 1 - 2\left(q_1^2 + q_2^2\right) \end{bmatrix}. \tag{4.37}$$

Let $\boldsymbol{\omega}$ denote the angular velocity of the spacecraft body fixed frame $\mathcal{F}_b$ relative to the inertial frame $\mathcal{F}_i$ expressed in the body frame. Then, the angular velocity of $\mathcal{F}_b$ relative to the orbital frame $\mathcal{F}_o$ can be written as

$$\boldsymbol{\omega}_r = \boldsymbol{\omega} + \dot{\eta}\boldsymbol{o}_2 = \boldsymbol{\omega} + n\boldsymbol{o}_2, \tag{4.38}$$

where $\boldsymbol{o}_2$ denotes the second column of the rotation matrix $\boldsymbol{C}$. The attitude kinematics can now be written in terms of quaternions as

$$\dot{\boldsymbol{q}} = \frac{1}{2}\left(q_4\boldsymbol{I} + \tilde{\boldsymbol{q}}\right)\boldsymbol{\omega}_r, \tag{4.39}$$

$$\dot{q}_4 = -\frac{1}{2}\boldsymbol{q}^T\boldsymbol{\omega}_r. \tag{4.40}$$

4.2.4 Gravity-Gradient Torque in Terms of Quaternions

The direction cosine matrix (3.42) can be written in terms of quaternions as

$$\begin{bmatrix} \hat{b}_1 \\ \hat{b}_2 \\ \hat{b}_3 \end{bmatrix} = \begin{bmatrix} 1-2(q_2^2+q_3^2) & 2(q_1q_2+q_3q_4) & 2(q_1q_3-q_2q_4) \\ 2(q_1q_2-q_3q_4) & 1-2(q_1^2+q_3^2) & 2(q_2q_3+q_1q_4) \\ 2(q_1q_3+q_2q_4) & 2(q_3q_2-q_1q_4) & 1-2(q_1^2+q_2^2) \end{bmatrix} \begin{bmatrix} \hat{o}_1 \\ \hat{o}_2 \\ \hat{o}_3 \end{bmatrix}. \tag{4.41}$$

The inertial angular velocity $\boldsymbol{\omega}$ of the spacecraft can be written in terms of quaternions as

$$\begin{bmatrix} \omega_1 \\ \omega_2 \\ \omega_3 \\ 0 \end{bmatrix} = 2\begin{bmatrix} q_4 & q_3 & q_2 & q_1 \\ -q_3 & q_4 & -q_1 & q_2 \\ q_2 & q_1 & q_4 & q_3 \\ q_1 & -q_2 & -q_3 & q_4 \end{bmatrix} \begin{bmatrix} \dot{q}_1 \\ \dot{q}_2 \\ \dot{q}_3 \\ \dot{q}_4 \end{bmatrix} - \begin{bmatrix} 2(q_1q_2+q_3q_4) \\ 1-2(q_1^2+q_3^2) \\ 2(q_3q_2-q_1q_4) \\ 0 \end{bmatrix}\dot{\eta}. \tag{4.42}$$

The gravity-gradient torque components M_i in the spacecraft body fixed frame $\mathcal{F}_b$ can be written in terms of quaternions as

$$\begin{aligned}
M_1 = \frac{\mu}{R_c^3}&[2(3+5\phi)(J_3 - J_2)(q_2q_3 + q_1q_4)\{1 - 2(q_1^2 + q_2^2)\} \\
&+ 5\chi(\frac{2}{5}J_1(q_1q_2 + q_3q_4) - (J_1 - J_2 + J_3)(q_1q_2 - q_3q_4)\{1 - 2(q_1^2 + q_2^2)\} \\
&+ (J_2 - J_3 + J_1)(q_1q_3 + q_2q_4)(q_2q_3 + q_1q_4))], \qquad (4.43) \\
M_2 = \frac{\mu}{R_c^3}&[2(3+5\phi)(J_1 - J_3)(q_1q_3 - q_2q_4)\{1 - 2(q_1^2 + q_2^2)\} \\
&+ \frac{5}{2}\chi(\frac{2}{5}J_2\{1 - 2(q_1^2 + q_3^2)\} + 4(J_2 - J_1 + J_3)(q_1q_3 + q_2q_4)(q_1q_3 - q_2q_4) \\
&- (J_2 - J_3 + J_1)\{1 - 2(q_2^2 + q_3^2)\}\{1 - 2(q_1^2 + q_2^2)\})], \qquad (4.44) \\
M_3 = \frac{\mu}{R_c^3}&[4(3+5\phi)(J_2 - J_1)(q_1q_3 - q_2q_4)(q_2q_3 + q_1q_4) \\
&+ 5\chi(\frac{2}{5}J_3(q_3q_2 - q_1q_4) - 2(J_2 - J_1 + J_3)(q_1q_2 - q_3q_4)(q_1q_3 - q_2q_4) \\
&+ (J_1 - J_2 + J_3)\{1 - 2(q_2^2 + q_3^2)\}(q_2q_3 + q_1q_4))]. \qquad (4.45)
\end{aligned}$$

4.2.5 Rotational Dynamics

We denote by $\boldsymbol{\tau}$ the control torque vector in the spacecraft body fixed frame $\mathcal{F}_b$. Then the attitude dynamics of the spacecraft can be expressed as

$$\boldsymbol{J}\dot{\boldsymbol{\omega}} + \tilde{\boldsymbol{\omega}}\boldsymbol{J}\boldsymbol{\omega} = \boldsymbol{\tau} + \boldsymbol{M}, \qquad (4.46)$$

where $\boldsymbol{M}$ is the gravity-gradient torque in the spacecraft body fixed frame $\mathcal{F}_b$ and $\boldsymbol{J}$ is the inertia matrix for the spacecraft, which is given by

$$\boldsymbol{J} = \begin{bmatrix} J_1 & 0 & 0 \\ 0 & J_2 & 0 \\ 0 & 0 & J_3 \end{bmatrix}. \qquad (4.47)$$

and $\tilde{\boldsymbol{\omega}}$ is the skew-symmetric matrix formed from $\boldsymbol{\omega}$:

$$\tilde{\boldsymbol{\omega}} = \begin{bmatrix} 0 & -\omega_3 & \omega_2 \\ \omega_3 & 0 & -\omega_1 \\ -\omega_2 & \omega_1 & 0 \end{bmatrix}. \tag{4.48}$$

Clearly, $\tilde{\boldsymbol{\omega}}\boldsymbol{J}\boldsymbol{\omega} = \boldsymbol{\omega} \times \boldsymbol{J}\boldsymbol{\omega}$ and, thus, both notations can be used interchangeably. Figures 4.11 displays the quaternions without the control torque. In the simulations, the initial angular velocities are given by

$$\omega_1(0) = \omega_2(0) = \omega_3(0) = 4 \times 10^{-5} \text{ rad/s}. \tag{4.49}$$

The initial quaternions for the spacecraft is given as follows:

$$[\boldsymbol{q}(0),\, q_4(0)] = [0.5,\, 0.5,\, 0.5,\, 0.5]^T. \tag{4.50}$$

For an uncontrolled rotational motion, the control torque $\boldsymbol{\tau}$ is set to be zero.

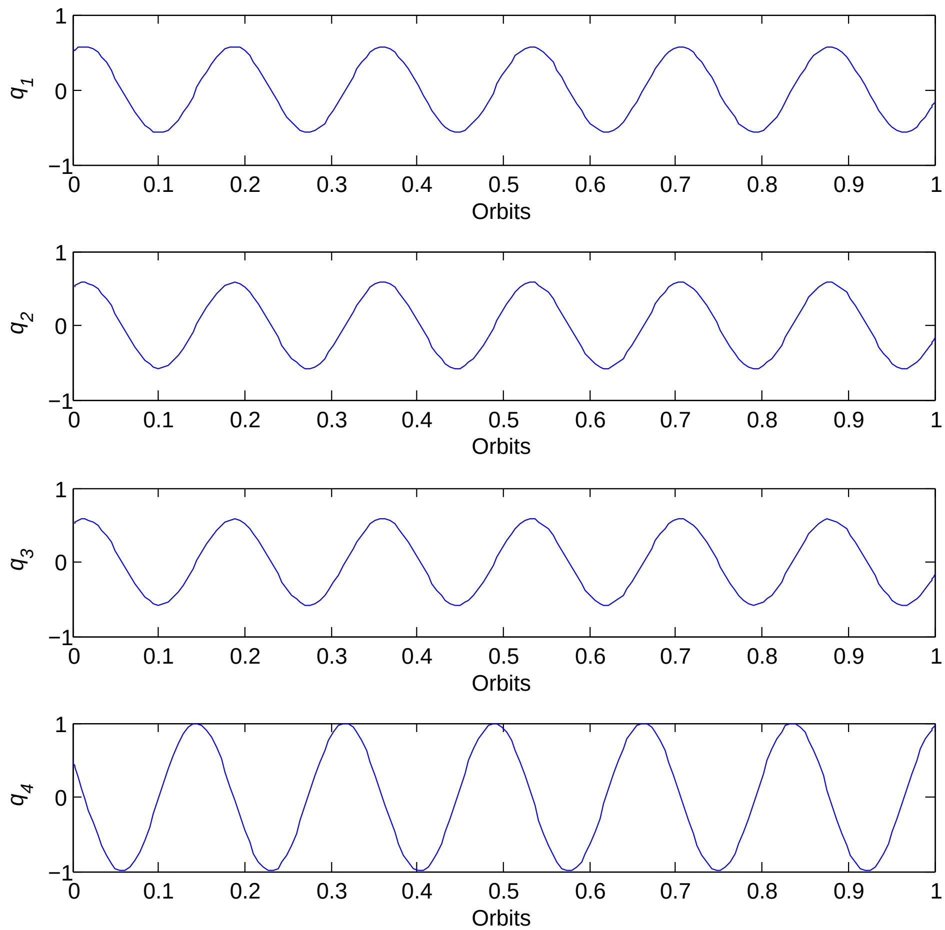

Figure 4.11: Quaternions for uncontrolled rotational motion.

Chapter 5

Translational and Rotational Control

This chapter is devoted to the design of translational and rotational feedback control laws. The control objective is to maintain a nadir pointing attitude on a circular equatorial orbit.

5.1 Translational Control Law

Consider the problem of asteroid-stationary orbit design for 433 EROS. The desired motion in the asteroid body fixed frame $\mathcal{F}_a$ is the equatorial motion and can be obtained as

$$\boldsymbol{R}^* = \begin{bmatrix} x^* \\ y^* \\ z^* \end{bmatrix} = \begin{bmatrix} R_c \cos(\dot{\eta} - \Omega)t \\ R_c \sin(\dot{\eta} - \Omega)t \\ 0 \end{bmatrix}, \tag{5.1}$$

$$\dot{\boldsymbol{R}}^* = \begin{bmatrix} \dot{x}^* \\ \dot{y}^* \\ \dot{z}^* \end{bmatrix} = \begin{bmatrix} -(\dot{\eta} - \Omega)y^* \\ (\dot{\eta} - \Omega)x^* \\ 0 \end{bmatrix}, \tag{5.2}$$

$$\ddot{\boldsymbol{R}}^* = \begin{bmatrix} \ddot{x}^* \\ \ddot{y}^* \\ \ddot{z}^* \end{bmatrix} = \begin{bmatrix} -(\dot{\eta} - \Omega)^2 x^* \\ -(\dot{\eta} - \Omega)^2 y^* \\ 0 \end{bmatrix}. \tag{5.3}$$

Here R_c denotes the radius of the circular orbit. The translational control problem is then to design a feedback control law such that, starting from any initial position $\boldsymbol{R}(0)$ and velocity $\dot{\boldsymbol{R}}(0)$, the spacecraft is driven to $\boldsymbol{R} = \boldsymbol{R}^*$ and $\dot{\boldsymbol{R}} = \dot{\boldsymbol{R}}^*$. The translational equation of motion of the spacecraft can be expressed as

$$\dot{\boldsymbol{R}} = \boldsymbol{V}, \tag{5.4}$$

$$\ddot{\boldsymbol{R}} = -2\boldsymbol{\Omega} \times \boldsymbol{V} - \boldsymbol{\Omega} \times (\boldsymbol{\Omega} \times \boldsymbol{R}) + \nabla U + \boldsymbol{F}/m, \tag{5.5}$$

where $\boldsymbol{F}$ denotes the translational control force in the asteroid body fixed frame. Define the error variables:

$$\begin{aligned} \boldsymbol{e} &= \boldsymbol{R} - \boldsymbol{R}^*, \\ \dot{\boldsymbol{e}} &= \dot{\boldsymbol{R}} - \dot{\boldsymbol{R}}^*, \\ \ddot{\boldsymbol{e}} &= \ddot{\boldsymbol{R}} - \ddot{\boldsymbol{R}}^*. \end{aligned} \tag{5.6}$$

Consider the following controller

$$\boldsymbol{F} = m\left(-\nabla U + 2\boldsymbol{\Omega} \times \boldsymbol{V}^* + \boldsymbol{\Omega} \times (\boldsymbol{\Omega} \times \boldsymbol{R}) - \boldsymbol{K}\boldsymbol{e} - \boldsymbol{C}\dot{\boldsymbol{e}} + \ddot{\boldsymbol{R}}^*\right), \tag{5.7}$$

where $\boldsymbol{C}$ and $\boldsymbol{K}$ are symmetric positive definite matrices. The closed-loop error dynamics are then given by

$$\ddot{\boldsymbol{e}} + \boldsymbol{C}\dot{\boldsymbol{e}} + \boldsymbol{K}\boldsymbol{e} + 2\boldsymbol{\Omega} \times \dot{\boldsymbol{e}} = 0. \tag{5.8}$$

To prove that the control law achieves the control objective, consider the following candidate Lyapunov function as introduced in sec 2.1,

$$E = \frac{1}{2}\dot{\boldsymbol{e}}^T\dot{\boldsymbol{e}} + \frac{1}{2}\boldsymbol{e}^T\boldsymbol{K}\boldsymbol{e}. \tag{5.9}$$

Taking the time derivative along the closed-loop trajectories yields

$$\dot{E} = \dot{\boldsymbol{e}}^T\ddot{\boldsymbol{e}} + \dot{\boldsymbol{e}}^T\boldsymbol{K}\boldsymbol{e} = -\dot{\boldsymbol{e}}^T\boldsymbol{C}\dot{\boldsymbol{e}}. \tag{5.10}$$

Clearly, $\dot{E} \leq 0$. Now it suffices to show that $\dot{E}$ is not identically zero along any solution of other than the desired equilibrium $\boldsymbol{e} = 0$, $\dot{\boldsymbol{e}} = 0$. It is easily seen that if the time derivative of the Lyapunov function is zero,

$$\dot{\boldsymbol{e}} \equiv 0 \qquad \Rightarrow \qquad \ddot{\boldsymbol{e}} \equiv 0, \tag{5.11}$$

which implies that

$$\boldsymbol{e} = 0 \tag{5.12}$$

as well, thus proving global asymptotic stability. This means that the proposed feedback control law drives the system to the desired equilibrium from any $\boldsymbol{e}(0)$ and $\dot{\boldsymbol{e}}(0)$. The feedback control law can be written in terms of original variables as

$$\boldsymbol{F} = m\left(-\nabla U + 2\boldsymbol{\Omega} \times \boldsymbol{V}^* + \boldsymbol{\Omega} \times (\boldsymbol{\Omega} \times \boldsymbol{R}) - \boldsymbol{K}(\boldsymbol{R} - \boldsymbol{R}^*) - \boldsymbol{C}(\boldsymbol{V} - \boldsymbol{V}^*) + \ddot{\boldsymbol{R}}^*\right). \tag{5.13}$$

The above feedback control force can be expressed in the spacecraft body fixed frame as

$$\boldsymbol{F} = \boldsymbol{C}\boldsymbol{C}_{ai}\boldsymbol{F}_a. \tag{5.14}$$

where $\boldsymbol{C}$ denotes the rotation matrix from the orbital frame to the spacecraft body fixed frame given by equation (4.37) and $\boldsymbol{C}_{ai}$ is the rotation matrix from the asteroid body fixed frame to the orbital frame given by

$$\boldsymbol{C}_{ai} = \begin{bmatrix} \cos\Omega t & \sin\Omega t & 0 \\ -\sin\Omega t & \cos\Omega t & 0 \\ 0 & 0 & 1 \end{bmatrix}. \tag{5.15}$$

5.2 Matlab Results

The translational control described above was simulated using Matlab's ode45 integrator; the control was applied in order to keep the spacecraft on a circular equatorial orbit of radius $R_c = 50$ km. Figure 5.7 shows the control forces in x, y, and z direction. The control force in z direction converges to zero by 0.005 orbits. Figures 5.1, 5.2, 5.3, 5.4, 5.5, and 5.6 show the results of the simulation that corresponds to initial conditions

$$\boldsymbol{R}(0) = [50,\ 5,\ 5]^T \text{ km}, \tag{5.16}$$

$$\dot{\boldsymbol{R}}(0) = [0.0001,\ -0.01355,\ 0.0001]^T \text{ km/s}. \tag{5.17}$$

Note that we set $m = 100$ kg, $\mu = 4.4631 \times 10^{-4}\text{km}^3/\text{s}^2$. The control gain matrices are

$$\boldsymbol{K} = \begin{bmatrix} 1 & 0 & 0 \\ 0 & 1 & 0 \\ 0 & 0 & 1 \end{bmatrix} \times 10^{-2}, \qquad \boldsymbol{C} = \begin{bmatrix} 2 & 0 & 0 \\ 0 & 2 & 0 \\ 0 & 0 & 2 \end{bmatrix} \times 10^{-2}. \tag{5.18}$$

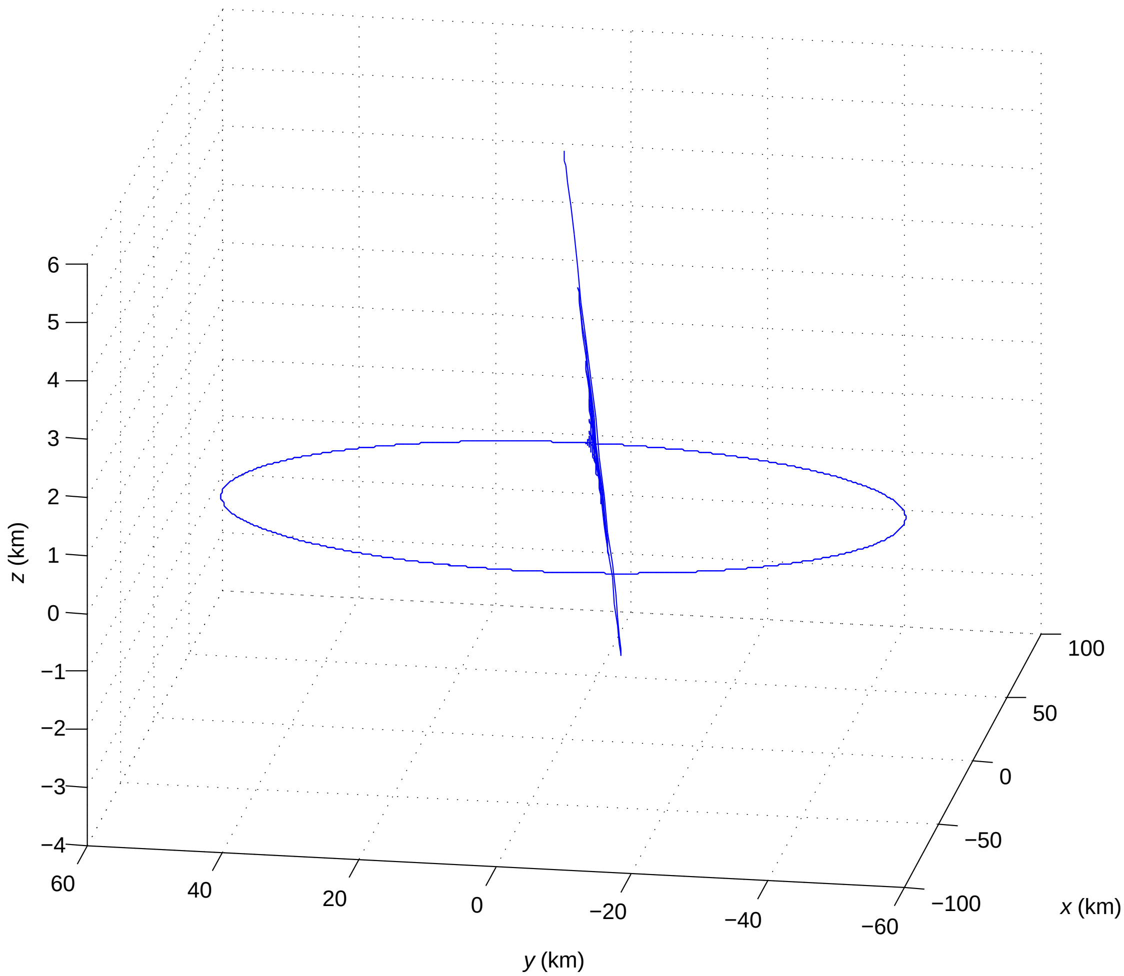

Figure 5.1: Three dimensional controlled spacecraft motion in the the asteroid frame ($R_c = 50$ km).

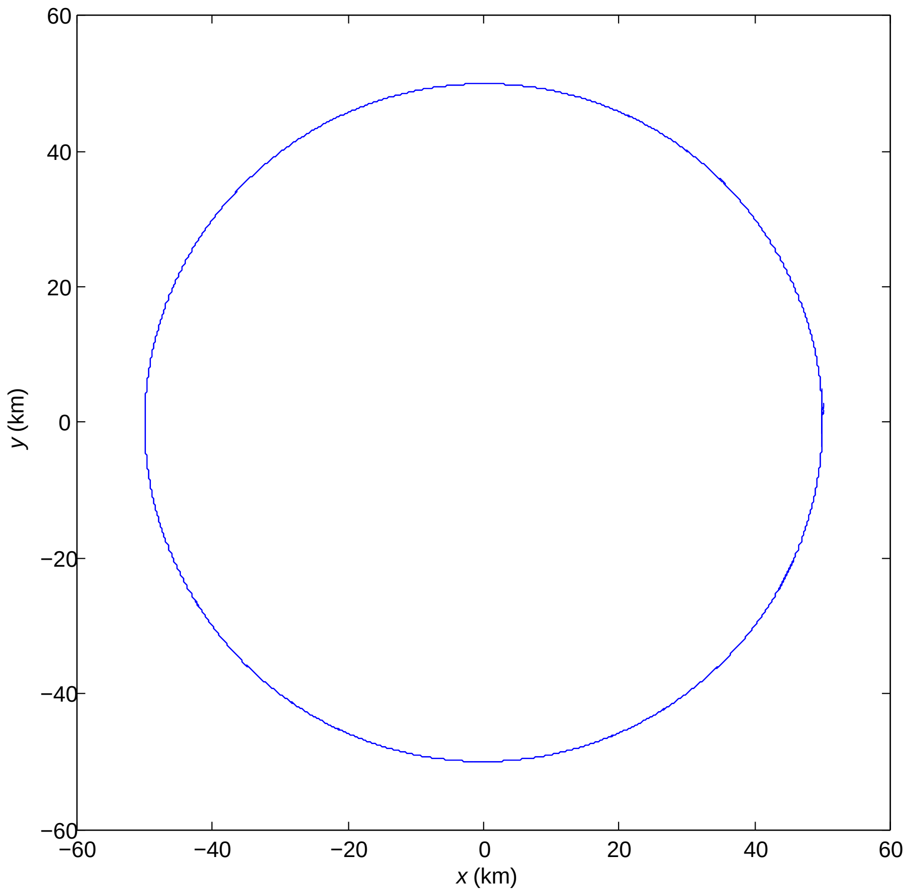

Figure 5.2: Two dimensional controlled spacecraft motion in the asteroid frame (R_c = 50 km).

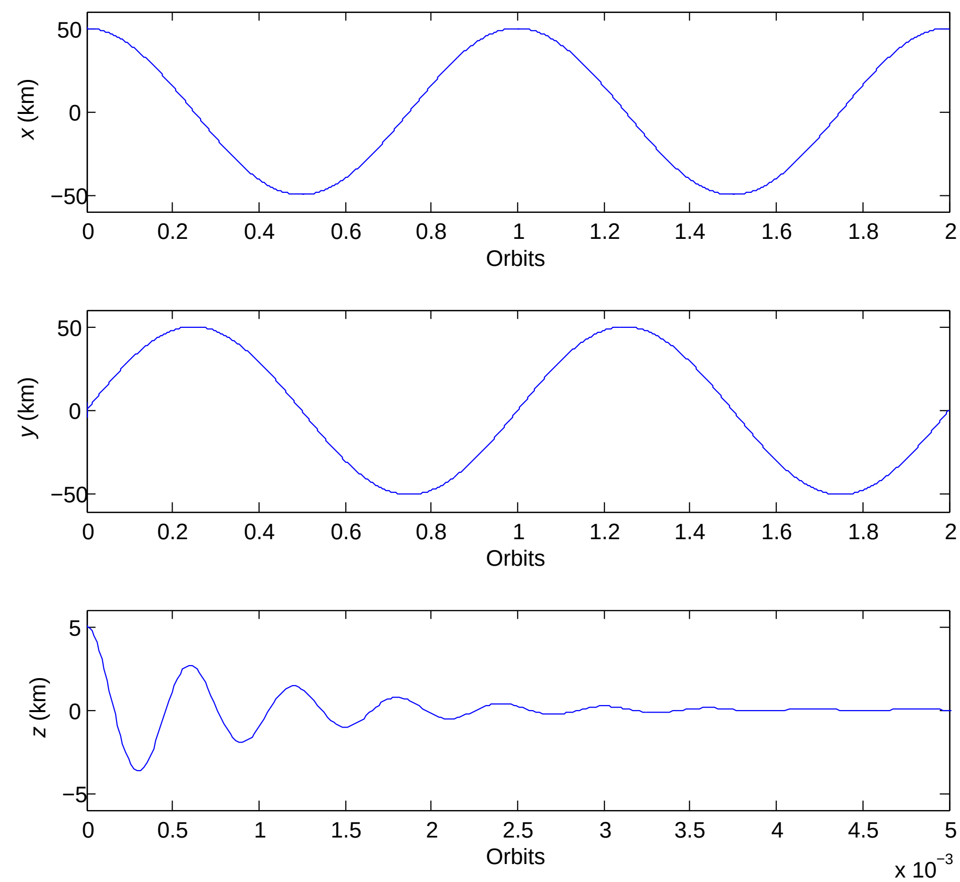

Figure 5.3: Controlled spacecraft x, y, and z positions ($R_c = 50$ km).

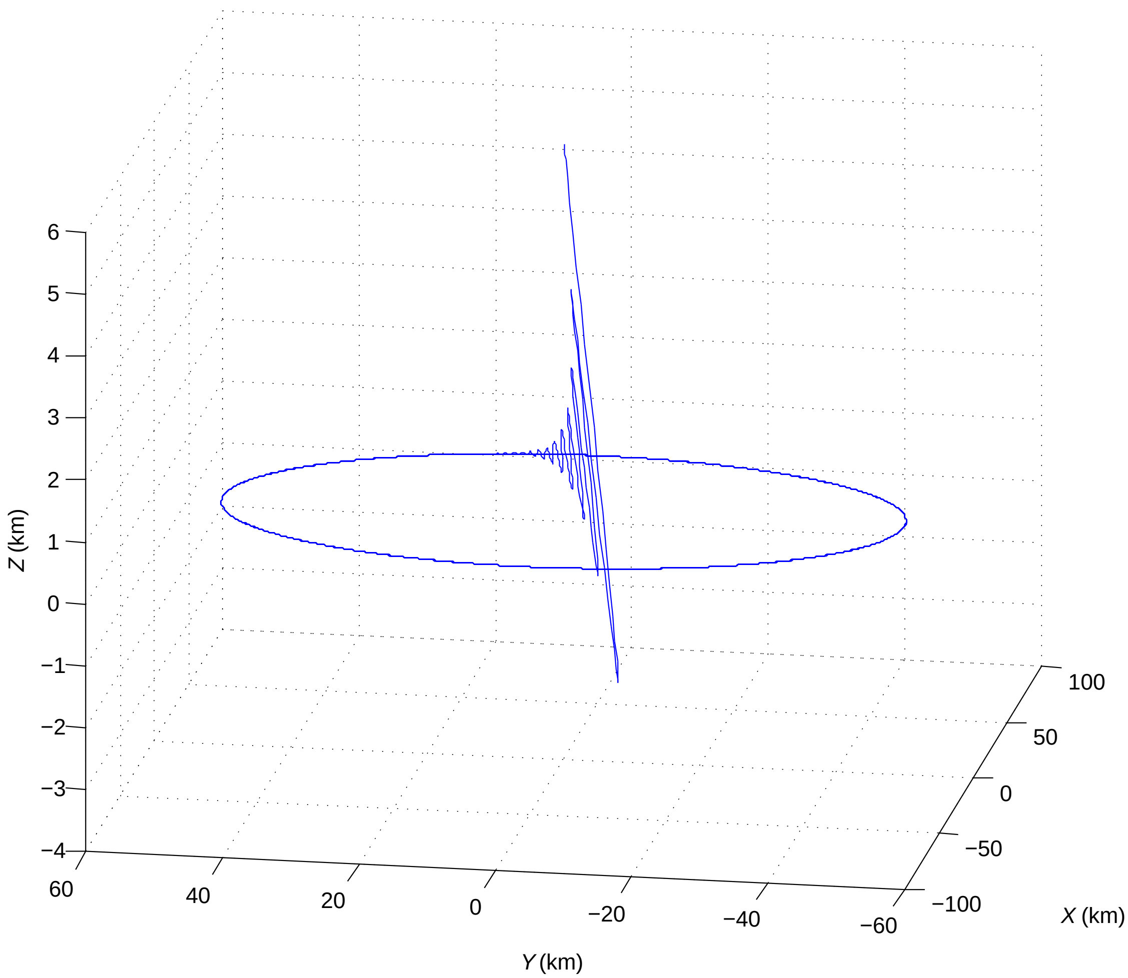

Figure 5.4: Three dimensional controlled spacecraft motion in the the inertial frame ($R_c = 50$ km).

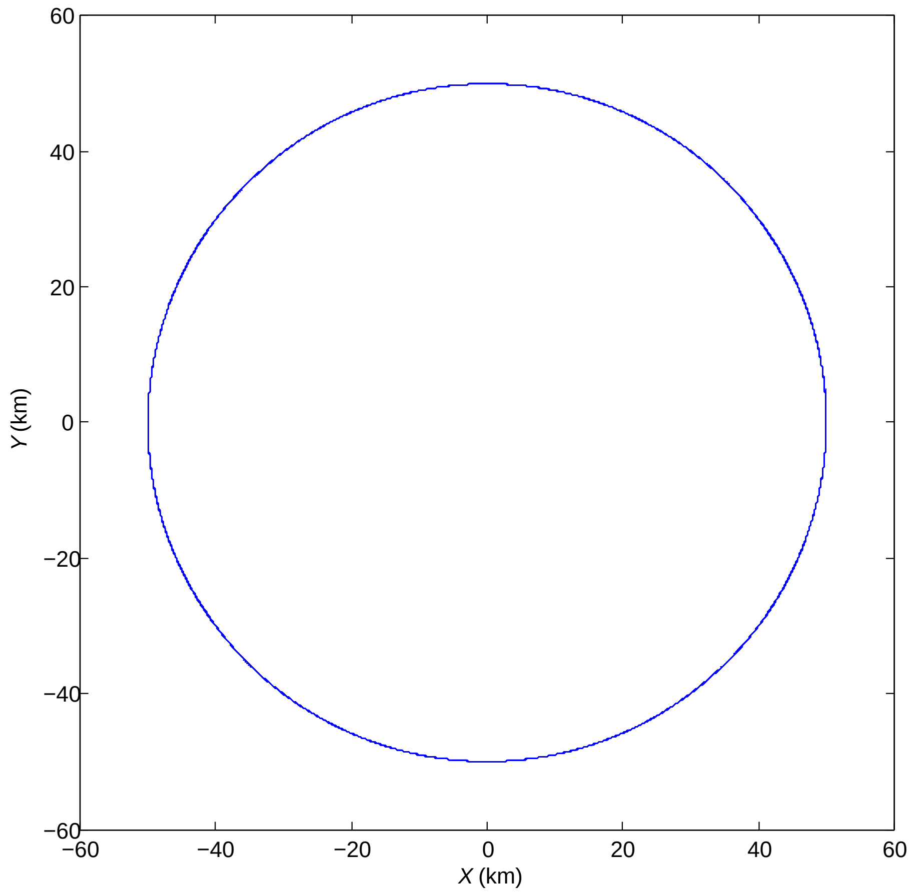

Figure 5.5: Two dimensional controlled spacecraft motion in the inertial frame (R_c = 50 km).

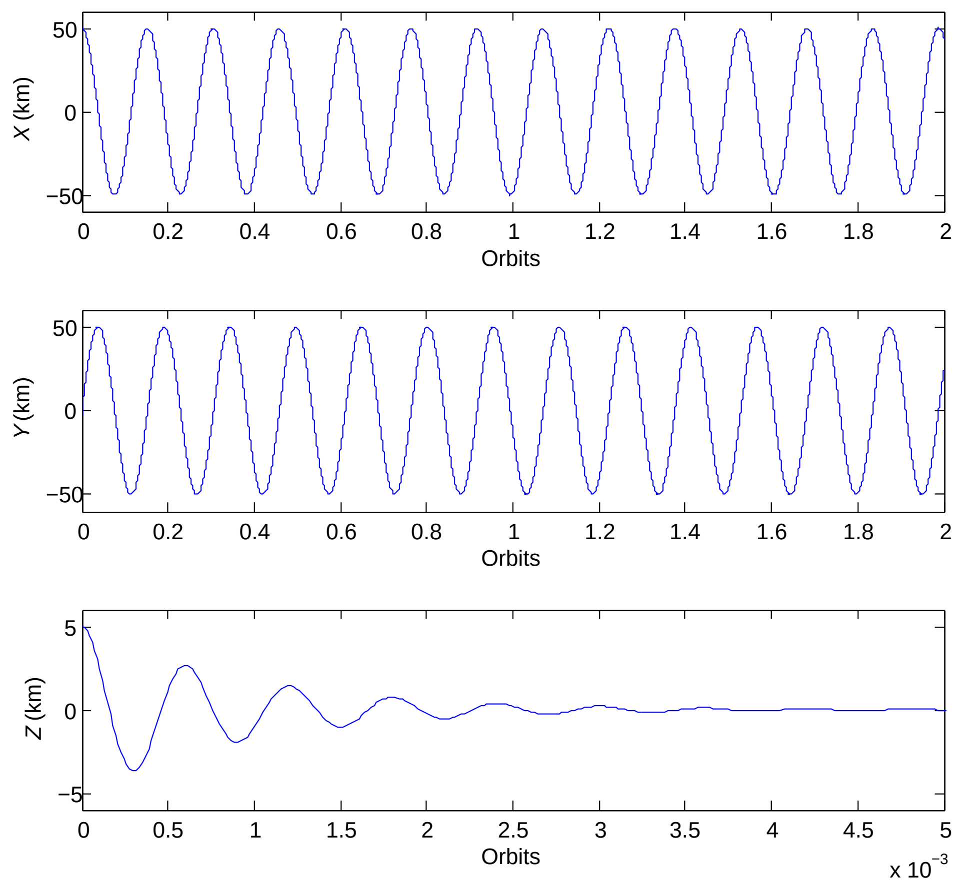

Figure 5.6: Controlled spacecraft X, Y, and Z positions ($R_c = 50$ km).

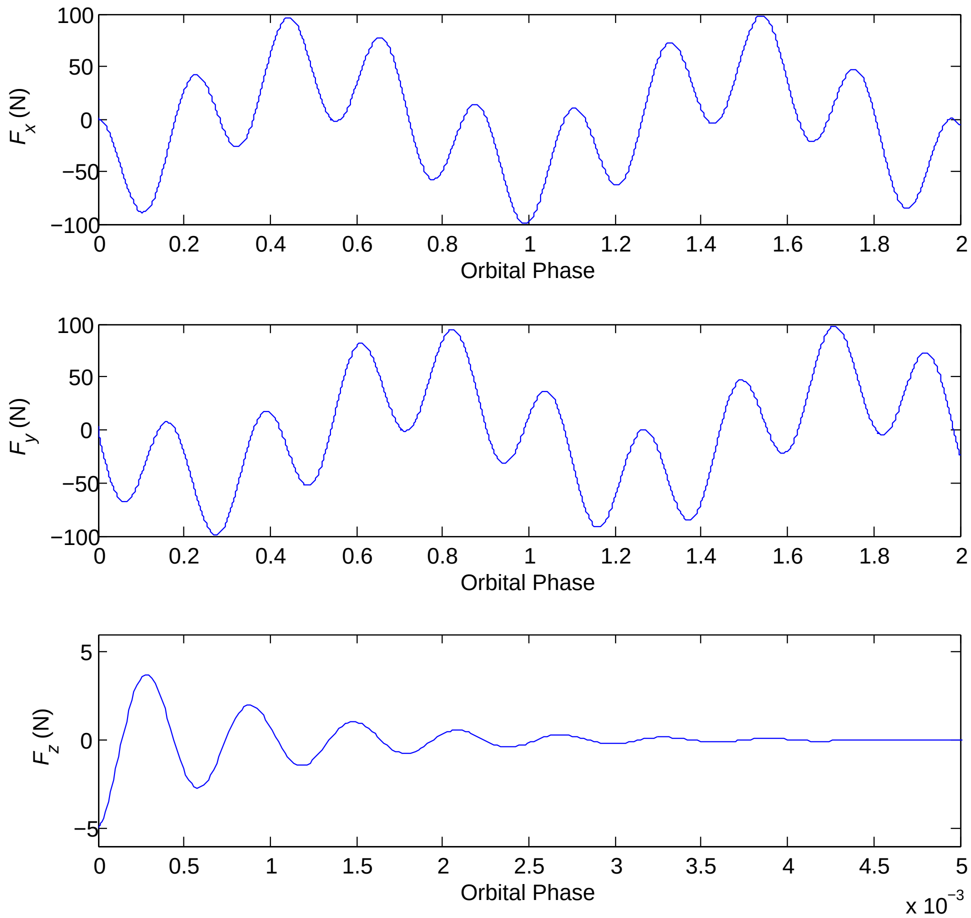

Figure 5.7: Control force F_a.

5.3 Rotational Control Law

In this section, we present a rotational feedback control law that achieves three-axis stabilized nadir-pointing attitude. In other words, the control objective is to align the spacecraft body fixed axes with the orbital reference axes. The desired attitude and angular velocity are given by $\boldsymbol{q}_d = 0,\ q_{4d} = 1,\ \boldsymbol{\omega}_d = -\dot{\eta}\boldsymbol{e}_2$, where $\mathbf{e}_2 = (0,\,1,\,0)^T$ is the second standard basis vector in $\mathbb{R}^3$. Let $\boldsymbol{\omega}_e = \boldsymbol{\omega} - \boldsymbol{\omega}_d$ denote the angular velocity error. Since $\boldsymbol{\omega}_d$ is constant, we have $\dot{\boldsymbol{\omega}}_e{=}\dot{\boldsymbol{\omega}}$. Now consider the rotational equations of motion for the spacecraft given by the equations (4.39), (4.40), and (4.46). It can be shown that the rotational equations of motion can be rewritten in terms of angular velocity error as

$$\boldsymbol{J}\dot{\boldsymbol{\omega}}_e + (\boldsymbol{\omega}_e + \boldsymbol{\omega}_d) \times \boldsymbol{J}(\boldsymbol{\omega}_e + \boldsymbol{\omega}_d) = \boldsymbol{\tau} + \boldsymbol{M}, \tag{5.19}$$

$$\dot{\boldsymbol{q}} = \frac{1}{2}\left(q_4\boldsymbol{\omega}_e - \boldsymbol{\omega}_e \times \boldsymbol{q}\right) + \boldsymbol{q} \times \boldsymbol{\omega}_d, \tag{5.20}$$

$$\dot{q}_4 = -\frac{1}{2}\boldsymbol{\omega}_e^T\boldsymbol{q}. \tag{5.21}$$

where $\boldsymbol{M}$ is the gravity gradient torque. The goal now is to design a feedback control $\boldsymbol{\tau}$ for the spacecraft to achieve the desired attitude and the desired angular velocity. Consider the following controller:

$$\boldsymbol{\tau} = -k\boldsymbol{J}\boldsymbol{q}_e - c\boldsymbol{J}\boldsymbol{\omega}_e + \boldsymbol{\omega} \times \boldsymbol{J}\boldsymbol{\omega} - \boldsymbol{M}, \tag{5.22}$$

where k and c are positive control parameters. The closed-loop dynamics can be written as

$$\dot{\boldsymbol{\omega}}_e = -k\boldsymbol{q} - c\boldsymbol{\omega}_e, \tag{5.23}$$

$$\dot{\boldsymbol{q}} = \frac{1}{2}\left(q_4\boldsymbol{\omega}_e - \boldsymbol{\omega}_e \times \boldsymbol{q}\right) + \boldsymbol{q} \times \boldsymbol{\omega}_e, \tag{5.24}$$

$$\dot{q}_{4e} = -\frac{1}{2}\boldsymbol{q}^T\boldsymbol{\omega}_e. \tag{5.25}$$

To prove that the control law (5.22) achieves the control objective, consider the following candidate Lyapunov function:

$$E = \frac{1}{2k}\boldsymbol{\omega}_e^T\boldsymbol{\omega}_e + \boldsymbol{q}^T\boldsymbol{q} + (q_4 - 1)^2. \tag{5.26}$$

The time derivative of E along the trajectories of this closed-loop system can be computed as

$$\dot{E} = \frac{\boldsymbol{\omega}_e^T\dot{\boldsymbol{\omega}}_e}{k} + 2\boldsymbol{q}^T\dot{\boldsymbol{q}} + 2(q_4 - 1)\dot{q}_4, \tag{5.27}$$

which simplifies to

$$\dot{E} = -\frac{c}{k}\boldsymbol{\omega}_e^T\boldsymbol{\omega}_e \leq 0. \tag{5.28}$$

Now it suffices to show that $\dot{E}$ is not identically zero along any solution of the equations (5.23)-(5.25) other than the desired equilibrium $\boldsymbol{\omega}_e = 0$. It can be easily seen that if the time derivative of the Lyapunov function is zero,

$$\boldsymbol{\omega}_e \equiv 0 \Rightarrow \dot{\boldsymbol{q}} = 0,\ \dot{q}_{4e} = 0,\ \dot{\boldsymbol{\omega}}_e = 0, \tag{5.29}$$

which implies

$$\boldsymbol{q} = 0, \qquad q_4 = 1, \tag{5.30}$$

as well, thus proving global asymptotic stability. This means that the proposed control law achieves the objective.

5.4 Matlab Results

To test the effectiveness of the previously discussed control scheme, Matlab was used to simulate the closed-loop response. The principal moments of inertias for the spacecraft are given by

$$\begin{aligned} J_1 &= 33 \text{ kg} \cdot \text{m}^2, \\ J_2 &= 33 \text{ kg} \cdot \text{m}^2, \\ J_3 &= 50 \text{ kg} \cdot \text{m}^2. \end{aligned} \tag{5.31}$$

In the simulations, the initial angular velocities are given by

$$\omega_1(0) = \omega_2(0) = \omega_3(0) = 4 \times 10^{-5} \text{ rad/s}. \tag{5.32}$$

The initial quaternions for the spacecraft is given as follows:

$$[\boldsymbol{q}(0),\, q_4(0)] = [0.5,\, 0.5,\, 0.5,\, 0.5]^T. \tag{5.33}$$

The control parameters are given by

$$k = 2, \qquad c = 1. \tag{5.34}$$

Figures 5.8 displays the spacecraft rotational motion in terms of quaternions. $\boldsymbol{q}$ goes to zero and q_4 goes to 1. It can be seen that the desired orbit is achieved. Figures 5.9 displays the control torque in the asteroid frame.

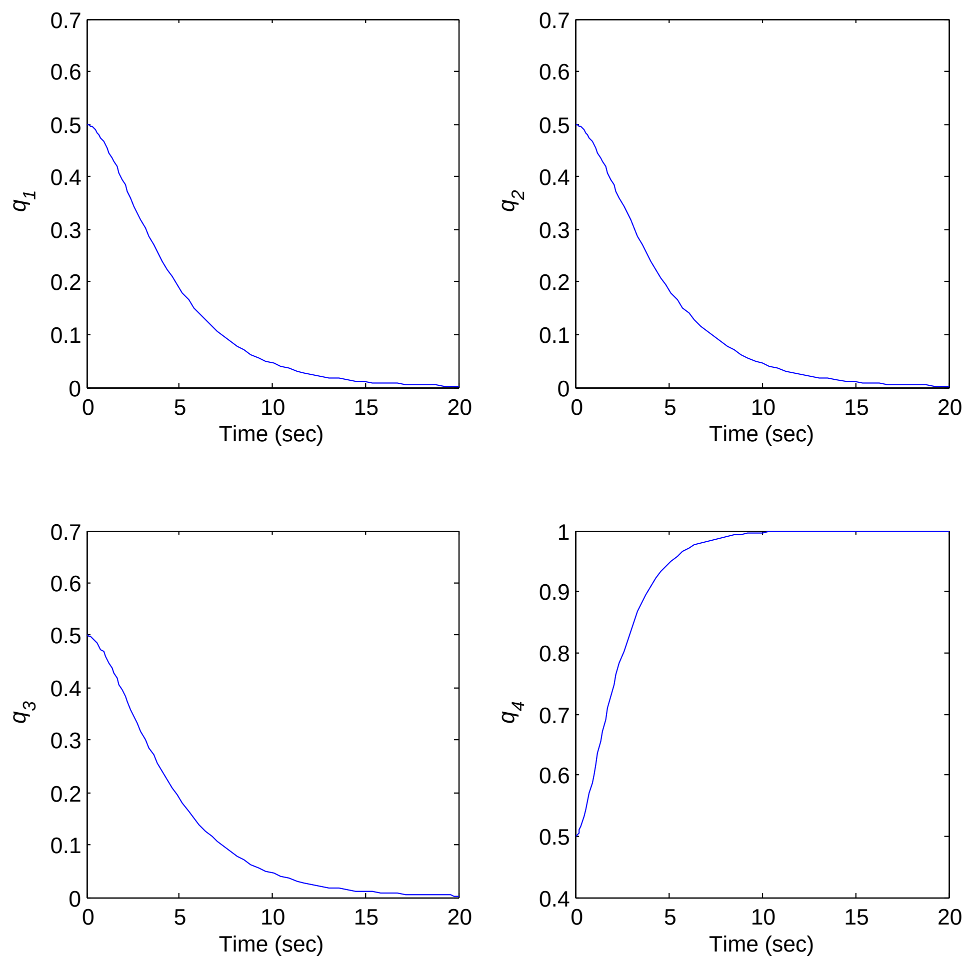

Figure 5.8: Quaternions for controlled rotational motion.

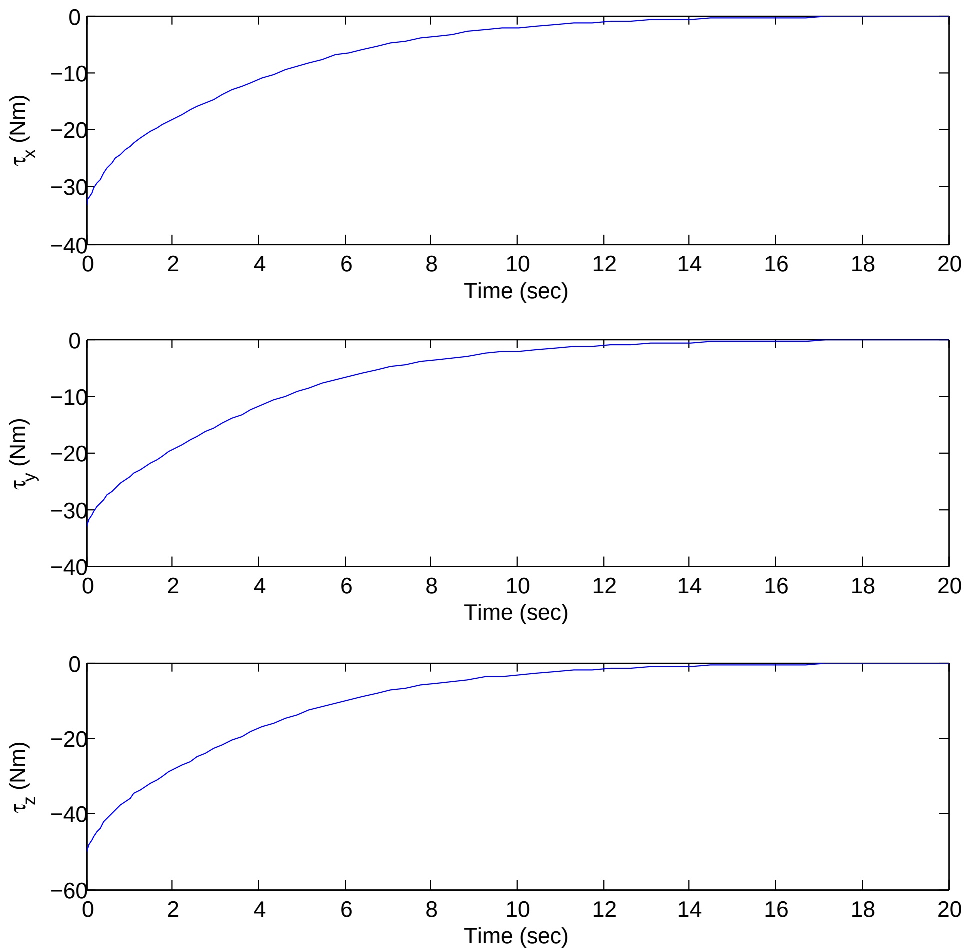

Figure 5.9: Control torque τ.

Chapter 6

Conclusions

This thesis has focused on the design of effective control algorithms for an asteroid orbiting spacecraft. The development has been carried out in particular for the asteroid 433 Eros. We have first summarized the progress made in the dynamics formulation of such spacecrafts and showed that the controlled motion of such spacecrafts would be adversely affected by the perturbation accelerations due to higher-order gravitational coefficients such as C_{20} and C_{22}. These terms characterize the oblateness and the equatorial ellipticity of the asteroid.

After presenting the gravitational force and gravity-gradient torque expressions for an asteroid, a theoretical framework has been developed for the control system design to maintain a nadir pointing attitude on a circular equatorial orbit. Using Lyapunov-based control design techniques, we have constructed feedback control laws to control both rotational and translational motion of the spacecraft to achieve the control objective. Computer simulations have been carried out to illustrate the effectiveness of the feedback control laws.

Chapter 7

Matlab Code

The code for the various simulations used in this thesis is given here.

7.1 Translational Motion MATLAB Code

7.1.1 Uncontrolled Translational Motion

```
%%%%%%%%%%%%%%%%%%%%%%%%%%%%%%%%%%%%%%%%%%%%%%%%%%%%%%%%%%%%%%%%%%%%%%%%%%%%%
% FUNCTION of Translational Motion without control law
%%%%%%%%%%%%%%%%%%%%%%%%%%%%%%%%%%%%%%%%%%%%%%%%%%%%%%%%%%%%%%%%%%%%%%%%%%%%%

function xx = WOCOrbitalFunction(t,x,Rc)
%% parameters
% gravitational parameter of 433 Eros
myu = 4.4631*10^-4;          % km^3 / s^2
% characteristic length of the asteroid
ro = 9.933;                  % km
% gravitational coefficients
C20 = -0.0878;
```

```
C22 = 0.0439;
% angular velocity of the asteroid
omega = 3.31 * 10^-4;        % rad / sec
% period of the asteroid
p = 2* pi / omega;           % sec
%velocity
v = sqrt(myu/Rc);            % km / sec
%the orbital rate
eta = v/Rc;                  % rad / sec
% longitude of the SC
lamda = (eta - omega)*t;     % rad

%% equation of motion
xx = [x(4);
    x(5);
    x(6);
    2*omega*x(5) + (omega^2)*x(1) ...
    - myu*x(1)*Rc^(-3)*(1 + 7.5*ro^2*C20*Rc^(-4)*x(3)^2 ...
    - 1.5*ro^2*C20*Rc^(-2) - 6*ro^2*C22*cos(2*lamda)*Rc^(-2) ...
    + 15*ro^2*C22*cos(2*lamda)*Rc^(-4)*(x(1)^2+x(2)^2));
    -2*omega*x(4) + (omega^2)*x(2) ...
    - myu*x(2)*Rc^(-3)* (1 + 7.5*ro^2*C20*Rc^(-4)*x(3)^2 ...
    - 1.5*ro^2*C20*Rc^(-2) - 6*ro^2*C22*cos(2*lamda)*Rc^(-2) ...
    + 15*ro^2*C22*cos(2*lamda)*Rc^(-4)*(x(1)^2+x(2)^2));
    - myu*x(3)*Rc^(-3)* (1 - 4.5*ro^2*C20*Rc^(-2) ...
    + 7.5*ro^2*C20*Rc^(-4)*x(3)^2 ...
    + 15*ro^2*C22*cos(2*lamda)*Rc^-4*(x(1)^2+x(2)^2))];

```

```
%%%%%%%%%%%%%%%%%%%%%%%%%%%%%%%%%%%%%%%%%%%%%%%%%%%%%%%%%%%%%%%%%%%%%%%%%%%
% SIMULATION of the translational motion without control law
%%%%%%%%%%%%%%%%%%%%%%%%%%%%%%%%%%%%%%%%%%%%%%%%%%%%%%%%%%%%%%%%%%%%%%%%%%%
clc
clear
close all

%% PARAMETERS
% Radius
Rc = 50;                        % km

% gravity parameter
myu = 4.4631*10^-4;             % km^3 / s^2
% velocity
v = sqrt(myu/Rc);               % km/sec
% orbital angular velocity
n = sqrt(myu/Rc^3);             % rad/sec
% asteroid rotation rate
omega = 3.31 * 10^(-4);         % rad/sec
% mass of the spacecraft
m = 100;                        % kg
% time period
T = 2*pi/n;                     % sec
% time span
ts = [0 2*T];                   % sec
%% initial conditions for position(x1,x2,x3) and velocities(x4,x5,x6)
x10 = Rc;                       % km
x20 = 0;                        % km
x30 = 0;                        % km
```

```
x40 = 0.0001;                % km/sec
x50 = -0.01355;              % km/sec
x60 = 0.0001;                % km/sec
% initial condition matrix
z0 = [x10 x20 x30 x40 x50 x60]';

%%  calculation in asteroid frame
[t, Q] = ode45(@(t,x) WOCOrbitalFunction(t,x,Rc), ts, z0);

for i = 1:length(t)
    x1 = Q(i,1);
    x2 = Q(i,2);
    x3 = Q(i,3);
    x4 = Q(i,4);
    x5 = Q(i,5);
    x6 = Q(i,6);
end

%% converting to the inertial frame
for i = 1:length(t)
    X1(i) = Q(i,1)*cos(omega*t(i)) - Q(i,2)*sin(omega*t(i));
    X2(i) = Q(i,1)*sin(omega*t(i)) + Q(i,2)*cos(omega*t(i));
    X3(i) = Q(i,3);
end

%% Plot
%% asteroid frame
% 2D xy plot
figure(1)
```

```
plot(Q(:,1),Q(:,2))
axis square
xlabel('{\it x} (km)')
ylabel('{\it y} (km)')
% x,y,z positions vs time
figure(2)
subplot(311)
plot(t/T,Q(:,1))
xlabel('Orbital Phase')
ylabel('{\it x} (km)')
subplot(312)
plot(t/T,Q(:,2))
xlabel('Orbital Phase')
ylabel('{\it y} (km)')
subplot(313)
plot(t/T,Q(:,3))
xlabel('Orbital Phase')
ylabel('{\it z} (km)')
% 3d plot
figure(3)
plot3(Q(:,1),Q(:,2),Q(:,3))
grid on
xlabel('{\it x} (km)')
ylabel('{\it y} (km)')
zlabel('{\it z} (km)')

%% inertial frame
% 2D XY plot
figure(4)
```

```
plot(X1,X2)
axis square
xlabel('{\it X} (km)')
ylabel('{\it Y} (km)')
% X,Y,Z positions vs time
figure(5)
subplot(311)
plot(t/T,X1)
xlabel('Orbital Phase')
ylabel('{\it X} (km)')
subplot(312)
plot(t/T,X2)
xlabel('Orbital Phase')
ylabel('{\it Y} (km)')
subplot(313)
plot(t/T,X3)
xlabel('Orbital Phase')
ylabel('{\it Z} (km)')
% 3d plot
figure(6)
plot3(X1,X2,X3)
grid on
xlabel('{\it X} (km)')
ylabel('{\it Y} (km)')
zlabel('{\it Z} (km)')
```

7.1.2 Controlled Translational Motion

```
%%%%%%%%%%%%%%%%%%%%%%%%%%%%%%%%%%%%%%%%%%%%%%%%%%%%%%%%%%%%%%%%%%%%%%%%%%%%%%%
% FUNCTION of the translational motion with control law
%%%%%%%%%%%%%%%%%%%%%%%%%%%%%%%%%%%%%%%%%%%%%%%%%%%%%%%%%%%%%%%%%%%%%%%%%%%%%%%

%% input variables
% Orbital Radius, Rc
% Control Parameters, k, c

function xx = ControlOrbitalFunction(t,x,Rc,k,c)
%% parameters
% gravitational
myu = 4.4631*10^-4;           % km^3 / s^2
% angular velocity of the asteroid
omega = 3.31 * 10^-4;         % rad / sec
%velocity
v = sqrt(myu/Rc);             % km/sec
% time derivative of true anomaly
n = sqrt(myu/Rc^3);           % rad / sec
% The desired position
xs = Rc*cos(n*t);             % km
ys = Rc*sin(n*t);             % km
% asteroid rotation rate
omega = 3.31 * 10^(-4);       % rad/sec
% The angle
lambda = (omega + n)*t;       % rad

%% equation of motion
```

```
xx = [x(4);
    x(5);
    x(6);
    -c*x(4)-k*x(1)+2*omega*x(5)-2*omega*n*xs+k*xs-c*n*ys-(n^2)*xs;
    -c*x(5)-k*x(2)-2*omega*x(4)-2*omega*n*ys+k*ys+c*n*xs-(n^2)*ys;
    -k*x(3)-c*x(6)];
```

```
%%%%%%%%%%%%%%%%%%%%%%%%%%%%%%%%%%%%%%%%%%%%%%%%%%%%%%%%%%%%%%%%%%%%%%%%%%%
% SIMULATION of the translational motion with control law
%%%%%%%%%%%%%%%%%%%%%%%%%%%%%%%%%%%%%%%%%%%%%%%%%%%%%%%%%%%%%%%%%%%%%%%%%%%
clc
clear
close all

%% Parameters
% Radius
Rc = 50;                        % km
% Control Parameters
k = 1*10^-2;
c = 2*10^-2;

% gravity parameter
myu = 4.4631*10^-4;             % km^3 / sec^2
% velocity
v = sqrt(myu/Rc);               % km/sec
% asteroid rotation rate
omega = 3.31 * 10^(-4);         % rad/sec
% time derivative of true anomaly
n = sqrt(myu/Rc^3);             % rad / sec
```

```
% time period
T = 2*pi/n                      % sec
Tm = T/60
Th = Tm/60
Td = Th/24
% time span
ts = [0 2*T];                   % sec

%% initial conditions for position(x1,x2,x3) and velocities(x4,x5,x6)
x10 = Rc;                       % km
x20 = 5;                        % km
x30 = 5;                        % km
x40 = 0.0001;                   % km/sec
x50 = v - omega*Rc;               % km/sec
x60 = 0.0001;                   % km/sec
% initial condition matrix
z0 = [x10 x20 x30 x40 x50 x60]';

%%  calculation in asteroid frame
[t, Q] = ode45(@(t,x) ControlOrbitalFunction(t,x,Rc,k,c), ts, z0);
for i = 1:length(t)
    x1 = Q(i,1);
    x2 = Q(i,2);
    x3 = Q(i,3);
    x4 = Q(i,4);
    x5 = Q(i,5);
    x6 = Q(i,6);
end

```

```
%% converting to the inertial frame
for i = 1:length(t)
    X1(i) = Q(i,1)*cos(omega*t(i)) - Q(i,2)*sin(omega*t(i));
    X2(i) = Q(i,1)*sin(omega*t(i)) + Q(i,2)*cos(omega*t(i));
    X3(i) = Q(i,3);
end

%% Plot
%--------------------------------------------------------------------------
% Asteroid Frame
% 2D plot x vs y
figure(1)
plot(Q(:,1),Q(:,2))
axis square
xlabel('{\it x} (km)')
ylabel('{\it y} (km)')
% x,y,z positions vs # of orbit
figure(2)
subplot(311)
plot(t/T,Q(:,1))
xlabel('Orbital Phase')
ylabel('{\it x} (km)')
subplot(312)
plot(t/T,Q(:,2))
xlabel('Orbital Phase')
ylabel('{\it y} (km)')
subplot(313)
plot(t/T,Q(:,3))
xlabel('Orbital Phase')
```

```
ylabel('{\it z} (km)')
% 3-D plot
figure(3)
plot3(Q(:,1),Q(:,2),Q(:,3))
grid on
xlabel('{\it x} (km)')
ylabel('{\it y} (km)')
zlabel('{\it z} (km)')
% z vs time
figure(4)
plot(t,Q(:,3))
xlabel('Time (sec)')
ylabel('{\it z} (km)')
%--------------------------------------------------------------------------
% Inertial Frame
% 2D plot X vs Y
figure(5)
plot(X1,X2)
axis square
xlabel('{\it X} (km)')
ylabel('{\it Y} (km)')
% X,Y,Z positions vs time
figure(6)
subplot(311)
plot(t/T,X1)
xlabel('Orbital Phase')
ylabel('{\it X} (km)')
subplot(312)
plot(t/T,X2)
```

```
xlabel('Orbital Phase')
ylabel('{\it Y} (km)')
subplot(313)
plot(t/T,X3)
xlabel('Orbital Phase')
ylabel('{\it Z} (km)')
% 3D plot
figure(7)
axis square
plot3(X1,X2,X3)
grid on
xlabel('{\it X} (km)')
ylabel('{\it Y} (km)')
zlabel('{\it Z} (km)')
% Z vs time
figure(8)
plot(t,X3)
xlabel('Time (sec)')
ylabel('{\it Z} (km)')
```

```
%%%%%%%%%%%%%%%%%%%%%%%%%%%%%%%%%%%%%%%%%%%%%%%%%%%%%%%%%%%%%%%%%%%%%%%%%%%
% SIMULATION of the control force (translational motion control)
%%%%%%%%%%%%%%%%%%%%%%%%%%%%%%%%%%%%%%%%%%%%%%%%%%%%%%%%%%%%%%%%%%%%%%%%%%%
clc
clear
close all

%% Parameters
% Radius
```

```
Rc = 50;                                % km
% Control Parameters
k = 1/100;
c = 2/100;
% gravity parameter
myu = 4.4631*10^(-4);                   % km^3 / sec^2
% velocity
v = sqrt(myu/Rc);                       % km/sec
% characteristic length
ro = 9.933;                             % km
% gravity harmonic parameters
C20 = -0.0878;
C22 = 0.0439;
% orbital angular velocity
n = sqrt(myu/Rc^3);                     % rad/sec
% asteroid rotation rate
omega = 3.31 * 10^(-4);                 % rad/sec
% mass of the spacecraft
m = 100;                                % kg
% time period
T = 2*pi/n;                             % sec
% time span
ts = [0 2*T];                           % sec
%% initial conditions for position(x1,x2,x3) and velocities(x4,x5,x6)
x10 = Rc;                               % km
x20 = 5;                                % km
x30 = 5;                                % km
x40 = 0.0001;                           % km/sec
x50 = v-omega*Rc;                       % km/sec
```

```
x60 = 0.0001;                          % km/sec
% initial condition matrix
z0 = [x10 x20 x30 x40 x50 x60]';

%%  calculation in asteroid frame
[t, Q] = ode45(@(t,x) ControlOrbitalFunction(t,x,Rc,k,c), ts, z0);
for i = 1:length(t)
    x1 = Q(i,1);
    x2 = Q(i,2);
    x3 = Q(i,3);
    x4 = Q(i,4);
    x5 = Q(i,5);
    x6 = Q(i,6);
end

%% Calculation of the control force Fa
% defining the new parameter l
l = n - omega;

for i = 1:length(t)
    % the distance A from CMa to SC
    A = Q(i,1)^2+Q(i,2)^2+Q(i,3)^2;
    % The angle
    lambda(i) = (omega + n)*t(i); % rad
    % control force
    Fa1(i) = m*(-myu*Q(i,1)*A^(-1.5)*(1 + 7.5*ro^2*C20*Q(i,3)^2*A^(-2) ...
    - 1.5*ro^2*C20*A^(-1) - 6*ro^2*C22*cos(2*lambda(i))*A^(-1) ...
    + 15*ro^2*C22*(Q(i,1)^2+Q(i,2)^2)*cos(2*lambda(i))*A^(-2)) ...
    - 2*Rc*omega*l*cos(l*t(i)) - (omega^2+k)*Q(i,1) + k*Rc*cos(l*t(i)) ...
```

```
    - c*Q(i,4) - c*Rc*l*sin(l*t(i)) - Rc*l^2*cos(l*t(i)));
    Fa2(i) = m*(-myu*Q(i,2)*A^(-1.5)*(1 + 7.5*ro^2*C20*Q(i,3)^2*A^(-2 ) ...
    - 1.5*ro^2*C20*A^(-1) - 6*ro^2*C22*cos(2*lambda(i))*A^(-1) ...
    + 15*ro^2*C22*(Q(i,1)^2+Q(i,2)^2)*cos(2*lambda(i))*A^(-2)) ...
    - 2*Rc*omega*l*sin(l*t(i)) - (omega^2+k)*Q(i,2) + k*Rc*sin(l*t(i)) ...
    - c*Q(i,5) + c*Rc*l*cos(l*t(i)) - Rc*l^2*sin(l*t(i)));
    Fa3(i) = m*(-myu*Q(i,3)*A^(-1.5)*(1 - 4.5*ro^2*C20*A^(-1) ...
    + 7.5*ro^2*C20*A^(-1) ...
    + 15*ro^2*C22*(Q(i,1)^2+Q(i,2)^2)*cos(2*lambda(i))*A^(-2)) ...
    - k*Q(i,3) - c*Q(i,6));
end

%% Plot
% Asteroid Frame
figure(1)
subplot(311)
plot(t/T,Fa1)
xlabel('Orbital Phase')
ylabel('{\it F_{x}} (N)')
subplot(312)
plot(t/T,Fa2)
xlabel('Orbital Phase')
ylabel('{\it F_{y}} (N)')
subplot(313)
plot(t/T,Fa3)
xlabel('Orbital Phase')
ylabel('{\it F_{z}} (N)')
```

7.2 Rotational Motion MATLAB Code

7.2.1 Uncontrolled Rotational Motion

```
%%%%%%%%%%%%%%%%%%%%%%%%%%%%%%%%%%%%%%%%%%%%%%%%%%%%%%%%%%%%%%%%%%%%%%%%%%%%
% FUNCTION of the rotational motion without control law in terms of
% quaternion
%%%%%%%%%%%%%%%%%%%%%%%%%%%%%%%%%%%%%%%%%%%%%%%%%%%%%%%%%%%%%%%%%%%%%%%%%%%%

%% input variables
% Orbital Radius, Rc

function Q = WOCRotationalFunction(t,x,Rc)

%% parameters
% Moment of inertia
J1 = 33;
J2 = 33;
J3 = 50;
J = [J1 0 0; 0 J2 0; 0 0 J3];
% The Gravit parameter of Eros
myu = 4.4631 * 10^(-4);          % km^3/sec^2
% the characteristic length
ro = 9.933;                      % km
% gravity hamonic parameter
C20 = -0.0878;
C22 = 0.0439;
% orbital angular velocity of the spacecraft
n = ((myu)/Rc^3)^0.5;            % rad/sec
```

```
% asteroid rotation rate
omega = 3.31 * 10^(-4);           % rad/sec
% the angle
lamda = (omega + n)*t;            % rad
% phi and xi
phi = (-3/2*C20+9*C22*cos(2*lamda))*(ro/Rc)^2;
xi = 6*C22*sin(2*lamda)*(ro/Rc)^2;

%% angular velocity
% current angular velocity
w = [x(5) x(6) x(7)]';            % rad/sec
% desired angular velocity
wd = [0 0 n]';                    % rad/sec
% angular velocity error
we = w - wd;                      % rad/sec

%% quaternion
% current quaternion
% q = [x(1) x(2) x(3) x(4)]';
% desired quaternion
qd = [0 0 sin(n*t/2) cos(n*t/2)]';
% error quaternion
qe = [qd(4)*x(1) + qd(3)*x(2);
    -qd(3)*x(1) + qd(4)*x(2);
    qd(4)*x(3) - qd(3)*x(4);
    qd(3)*x(3) + qd(4)*x(4)];

%% Gravity Gradient Torque
M1 = (myu/Rc^3)*((6+10*phi)*(J3-J2)*(x(2)*x(3) ...
```

```
+ x(1)*x(4))*(1-2*(x(1)*x(1) + x(2)*x(2))) ...
+ 5*xi*(2/5*J1*(x(1)*x(2)+x(3)*x(4)) ...
+ (J1-J3+J2)*(x(1)*x(2)-x(3)*x(4))*(1-2*(x(1)*x(1)+x(2)*x(2))) ...
- 2* (J3-J2+J1)*(x(1)*x(3)+x(2)*x(4))*(x(3)*x(2)+x(1)*x(4))));
M2 = (myu/Rc^3)*((6+10*phi)*(J1-J3)*(x(1)*x(3)-x(2)*x(4)) ...
*(1-2*(x(1)*x(1)+ x(2)*x(2))) ...
+ 5/2*xi*(2/5*J2*(1-2*(x(1)*x(1)+x(3)*x(3))) ...
+ 4*(J2-J1+J3)*(x(1)*x(3)+x(2)*x(4))*(x(1)*x(3)-x(2)*x(4)) ...
- (J2-J3+J1)*(1-2*(x(2)*x(2)+x(3)*x(3)))*(1-2*(x(1)*x(1)+x(2)*x(2)))));
M3 = (myu/Rc^3)*((12+20*phi)*(J2-J1)*(x(1)*x(3)-x(2)*x(4)) ...
*(x(2)*x(3)+x(1)*x(4)) ...
+ 5*xi*(2/5*J3*(x(2)*x(3)-x(1)*x(4)) ...
- 2*(J2-J1+J3)*(x(1)*x(2)-x(3)*x(4))*(x(1)*x(3)-x(2)*x(4)) ...
+ (J1-J2+J3)*(1-2*(x(2)*x(2)+x(3)*x(3)))*(x(2)*x(3)+x(1)*x(4))));

% differential equations
Q = [0.5*(x(4)*x(5) - x(6)*x(3) + x(7)*x(2));
      0.5*(x(4)*x(6) - x(7)*x(1) + x(5)*x(3));
      0.5*(x(4)*x(7) - x(5)*x(2) + x(6)*x(1));
     -0.5*(x(5)*x(1) + x(6)*x(2) + x(7)*x(3));
     M1/J1;
     M2/J2;
     M3/J3];
```

```
%%%%%%%%%%%%%%%%%%%%%%%%%%%%%%%%%%%%%%%%%%%%%%%%%%%%%%%%%%%%%%%%%%%%%%%%%%%%
% SIMULATION of the Rotational Motion without control law in terms of
% quaternion
%%%%%%%%%%%%%%%%%%%%%%%%%%%%%%%%%%%%%%%%%%%%%%%%%%%%%%%%%%%%%%%%%%%%%%%%%%%%
clc
```

```
clear
close all

%% Parameters
% Radius
Rc = 50;                % km

% gravity parameter
myu = 4.4631*10^-4;     % km^3 / sec^2
% orbital angular velocity
n = sqrt(myu/Rc^3);     % rad/sec
% asteroid rotation rate
omega = 3.31 * 10^(-4); % rad/sec
% mass of the spacecraft
m = 100;                % kg
% time period
T = 2*pi/n;             % sec
% time span
ts = [0 T];             % sec

%% initial conditions
% quaternions(x1,x2,x3) and angular velocities(x4,x5,x6)
x10 = 0.5;
x20 = 0.5;
x30 = 0.5;
x40 = 0.5;
x50 = 4*10^(-4);
x60 = 4*10^(-4);
x70 = 4*10^(-4);
```

```
% initial condition matrix
z0 = [x10 x20 x30 x40 x50 x60 x70]';

%%  calculation in asteroid frame
[t, Q] = ode45(@(t,x) WOCRotationalFunction(t,x,Rc), ts, z0);

for i = 1:length(t)
    x1 = Q(i,1);
    x2 = Q(i,2);
    x3 = Q(i,3);
    x4 = Q(i,4);
    x5 = Q(i,5);
    x6 = Q(i,6);
    x7 = Q(i,7);
end

theta = 2*acos(Q(:,4));

%% plot
% q1
subplot(411)
plot(t/T,Q(:,1))
xlabel('Orbital Phase')
ylabel('{\it q_1}')
% q2
subplot(412)
plot(t/T,Q(:,2))
xlabel('Orbital Phase')
ylabel('{\it q_2}')
```

```
% q3
subplot(413)
plot(t/T,Q(:,3))
xlabel('Orbital Phase')
ylabel('{\it q_3}')
% q4
subplot(414)
plot(t/T,Q(:,4))
xlabel('Orbital Phase')
ylabel('{\it q_4}')
```

7.2.2 Controlled Rotational Motion

```
%%%%%%%%%%%%%%%%%%%%%%%%%%%%%%%%%%%%%%%%%%%%%%%%%%%%%%%%%%%%%%%%%%%%%%%%%%%%%
% FUNCTION of the rotational motion with control law
%%%%%%%%%%%%%%%%%%%%%%%%%%%%%%%%%%%%%%%%%%%%%%%%%%%%%%%%%%%%%%%%%%%%%%%%%%%%%

%% input variables
% Orbital Radius, Rc
% Control Parameters, k, c

function Q = ControlRotationalFunction(t,x,Rc,c,k)

% Moment of inertia
J1 = 33;
J2 = 33;
J3 = 50;
J = [J1 0 0; 0 J2 0; 0 0 J3];
```

```
% The Gravit parameter of Eros
myu = 4.4631 * 10^(-4);          % km^3/sec^2
% the characteristic length
ro = 9.933;                      % km
% gravity hamonic parameter
C20 = -0.0878;
C22 = 0.0439;
% orbital angular velocity of the spacecraft
n = ((myu)/Rc^3)^0.5;            % rad/sec
%% angular velocity
% current angular velocity
w = [x(5) x(6) x(7)]';           % rad/sec
% desired angular velocity
wd = [0 0 n]';                   % rad/sec
% angular velocity error
we = w - wd;                     % rad/sec

% asteroid rotation rate
omega = 3.31 * 10^(-4);          % rad/sec
%the angle
lamda = (omega + n)*t;           % rad
% phi and xi
phi = (-3/2*C20+9*C22*cos(2*lamda))*(ro/Rc)^2;
xi = 6*C22*sin(2*lamda)*(ro/Rc)^2;

%% quaternion
% current quaternion
%q = [x(1) x(2) x(3) x(4)]';
% desired quaternion
```

```
qd = [0 0 sin(n*t/2) cos(n*t/2)]';
% error quaternion
qe = [qd(4)*x(1) + qd(3)*x(2);
     -qd(3)*x(1) + qd(4)*x(2);
     qd(4)*x(3) - qd(3)*x(4);
     qd(3)*x(3) + qd(4)*x(4)];

%% Gravity Gradient Torque
M1 = (myu/Rc^3)*((6+10*phi)*(J3-J2)*(x(2)*x(3) ...
+ x(1)*x(4))*(1-2*(x(1)*x(1)+ x(2)*x(2))) ...
+ 5*xi*(2/5*J1*(x(1)*x(2)+x(3)*x(4)) ...
+ (J1-J3+J2)*(x(1)*x(2)-x(3)*x(4))*(1-2*(x(1)*x(1)+x(2)*x(2))) ...
- 2* (J3-J2+J1)*(x(1)*x(3)+x(2)*x(4))*(x(3)*x(2)+x(1)*x(4))));
M2 = (myu/Rc^3)*((6+10*phi)*(J1-J3)*(x(1)*x(3)-x(2)*x(4)) ...
*(1-2*(x(1)*x(1)+ x(2)*x(2))) ...
+ 5/2*xi*(2/5*J2*(1-2*(x(1)*x(1)+x(3)*x(3))) ...
+ 4*(J2-J1+J3)*(x(1)*x(3)+x(2)*x(4))*(x(1)*x(3)-x(2)*x(4)) ...
- (J2-J3+J1)*(1-2*(x(2)*x(2)+x(3)*x(3)))*(1-2*(x(1)*x(1)+x(2)*x(2)))));
M3 = (myu/Rc^3)*((12+20*phi)*(J2-J1)*(x(1)*x(3)-x(2)*x(4)) ...
*(x(2)*x(3)+x(1)*x(4)) + 5*xi*(2/5*J3*(x(2)*x(3)-x(1)*x(4)) ...
- 2*(J2-J1+J3)*(x(1)*x(2)-x(3)*x(4))*(x(1)*x(3)-x(2)*x(4)) ...
+ (J1-J2+J3)*(1-2*(x(2)*x(2)+x(3)*x(3)))*(x(2)*x(3)+x(1)*x(4))));

% differential equations
Q = [0.5*(x(4)*x(5) - x(6)*x(3) + x(7)*x(2));
      0.5*(x(4)*x(6) - x(7)*x(1) + x(5)*x(3));
      0.5*(x(4)*x(7) - x(5)*x(2) + x(6)*x(1));
     -0.5*(x(5)*x(1) + x(6)*x(2) + x(7)*x(3));
     -k*qe(1) - c*x(5) + M1/J1;
```

```
    -k*qe(2) - c*x(6) + M2/J2;
    -k*qe(3) - c*(x(7)-n) + M3/J3];

```

```
%%%%%%%%%%%%%%%%%%%%%%%%%%%%%%%%%%%%%%%%%%%%%%%%%%%%%%%%%%%%%%%%%%%%%%%%%%%%
% FUNCTION of the rotational motion with control law
%%%%%%%%%%%%%%%%%%%%%%%%%%%%%%%%%%%%%%%%%%%%%%%%%%%%%%%%%%%%%%%%%%%%%%%%%%%%

%% input variables
% Orbital Radius, Rc
% Control Parameters, k, c

function Q = ControlRotationalFunction(t,x,Rc,c,k)

% Moment of inertia
J1 = 33;
J2 = 33;
J3 = 50;
J = [J1 0 0; 0 J2 0; 0 0 J3];
% The Gravit parameter of Eros
myu = 4.4631 * 10^(-4);          % km^3/sec^2
% the characteristic length
ro = 9.933;                       % km
% gravity hamonic parameter
C20 = -0.0878;
C22 = 0.0439;
% orbital angular velocity of the spacecraft
n = ((myu)/Rc^3)^0.5;            % rad/sec
%% angular velocity
```

```
% current angular velocity
w = [x(5) x(6) x(7)]';           % rad/sec
% desired angular velocity
wd = [0 0 n]';                   % rad/sec
% angular velocity error
we = w - wd;                     % rad/sec

% asteroid rotation rate
omega = 3.31 * 10^(-4);          % rad/sec
%the angle
lamda = (omega + n)*t;           % rad
% phi and xi
phi = (-3/2*C20+9*C22*cos(2*lamda))*(ro/Rc)^2;
xi = 6*C22*sin(2*lamda)*(ro/Rc)^2;

%% quaternion
% current quaternion
%q = [x(1) x(2) x(3) x(4)]';
% desired quaternion
qd = [0 0 sin(n*t/2) cos(n*t/2)]';
% error quaternion
qe = [qd(4)*x(1) + qd(3)*x(2);
    -qd(3)*x(1) + qd(4)*x(2);
    qd(4)*x(3) - qd(3)*x(4);
    qd(3)*x(3) + qd(4)*x(4)];

%% Gravity Gradient Torque
M1 = (myu/Rc^3)*((6+10*phi)*(J3-J2)*(x(2)*x(3) ...
+ x(1)*x(4))*(1-2*(x(1)*x(1)+ x(2)*x(2))) ...
```

```
+ 5*xi*(2/5*J1*(x(1)*x(2)+x(3)*x(4)) ...
+ (J1-J3+J2)*(x(1)*x(2)-x(3)*x(4))*(1-2*(x(1)*x(1)+x(2)*x(2))) ...
- 2* (J3-J2+J1)*(x(1)*x(3)+x(2)*x(4))*(x(3)*x(2)+x(1)*x(4))));
M2 = (myu/Rc^3)*((6+10*phi)*(J1-J3)*(x(1)*x(3)-x(2)*x(4)) ...
*(1-2*(x(1)*x(1)+ x(2)*x(2))) ...
+ 5/2*xi*(2/5*J2*(1-2*(x(1)*x(1)+x(3)*x(3))) ...
+ 4*(J2-J1+J3)*(x(1)*x(3)+x(2)*x(4))*(x(1)*x(3)-x(2)*x(4)) ...
- (J2-J3+J1)*(1-2*(x(2)*x(2)+x(3)*x(3)))*(1-2*(x(1)*x(1)+x(2)*x(2)))));
M3 = (myu/Rc^3)*((12+20*phi)*(J2-J1)*(x(1)*x(3)-x(2)*x(4)) ...
*(x(2)*x(3)+x(1)*x(4)) + 5*xi*(2/5*J3*(x(2)*x(3)-x(1)*x(4)) ...
- 2*(J2-J1+J3)*(x(1)*x(2)-x(3)*x(4))*(x(1)*x(3)-x(2)*x(4)) ...
+ (J1-J2+J3)*(1-2*(x(2)*x(2)+x(3)*x(3)))*(x(2)*x(3)+x(1)*x(4))));

% differential equations
Q = [0.5*(x(4)*x(5) - x(6)*x(3) + x(7)*x(2));
     0.5*(x(4)*x(6) - x(7)*x(1) + x(5)*x(3));
     0.5*(x(4)*x(7) - x(5)*x(2) + x(6)*x(1));
    -0.5*(x(5)*x(1) + x(6)*x(2) + x(7)*x(3));
    -k*qe(1) - c*x(5) + M1/J1;
    -k*qe(2) - c*x(6) + M2/J2;
    -k*qe(3) - c*(x(7)-n) + M3/J3];

```

```
%%%%%%%%%%%%%%%%%%%%%%%%%%%%%%%%%%%%%%%%%%%%%%%%%%%%%%%%%%%%%%%%%%%%%%%%%%%%%
% SIMULATION of the Control Torque of the Rotational Motion
%%%%%%%%%%%%%%%%%%%%%%%%%%%%%%%%%%%%%%%%%%%%%%%%%%%%%%%%%%%%%%%%%%%%%%%%%%%%%
clc
clear
close all
```

```
%%  PARAMETERS
% Radius
Rc = 50;                        % km
% Control Parameters
k = 2;
c = 1;
% time span
ts = [0 20];                    % sec

% Moment of inertia
J1 = 33;
J2 = 33;
J3 = 50;
J = [J1 0 0; 0 J2 0; 0 0 J3];
% The Gravit parameter of Eros
myu = 4.4631 * 10^(-4);         % km^3/sec^2
% the characteristic length
ro = 9.933;                     % km
% gravity hamonic parameter
C20 = -0.0878;
C22 = 0.0439;
% orbital angular velocity of the spacecraft
n = ((myu)/Rc^3)^0.5;           % rad/sec

%% initial conditions for quaternions(x1,x2,x3)
% and angular velocities(x4,x5,x6)
x10 = 0.5;
x20 = 0.5;
```

```
x30 = 0.5;
x40 = 0.5;
x50 = 4*10^(-4);                % rad/sec
x60 = 4*10^(-4);                % rad/sec
x70 = 4*10^(-4);                % rad/sec
% initial condition matrix
z0 = [x10 x20 x30 x40 x50 x60 x70]';

%%  calculation in asteroid frame
[t, Q] = ode45(@(t,x) ControlRotationalFunction(t,x,Rc,k,c), ts, z0);

for i = 1:length(t)
    x1 = Q(i,1);
    x2 = Q(i,2);
    x3 = Q(i,3);
    x4 = Q(i,4);
    x5 = Q(i,5);
    x6 = Q(i,6);
    x7 = Q(i,7);
end

%% Calculate the Control Torque
% asteroid rotation rate
omega = 3.31 * 10^(-4);         % rad/sec

for i = 1:length(t)
    %the angle
    lambda(i) = (omega + n)*t(i);          % rad
    phi(i) = (-3/2*C20+9*C22*cos(2*lambda(i)))*(ro/Rc)^2;
```

```
    xi(i) = 6*C22*sin(2*lambda(i))*(ro/Rc)^2;
    %% quaternion
    % q = [Q(i,1) Q(i,2) Q(i,3)];
    % q4 = Q(i,4);
    % desired quaternion
    qd = [0 0 sin(n*t(i)/2) cos(n*t(i)/2)]';
    % error quaternion
    qe = [qd(4)*Q(i,1) + qd(3)*Q(i,2);
        -qd(3)*Q(i,1) + qd(4)*Q(i,2);
        qd(4)*Q(i,3) - qd(3)*Q(i,4)];
    qe4 = qd(3)*Q(i,3) + qd(4)*Q(i,4);
    %% angular velocity
    % current angular velocity
    w = [Q(i,5) Q(i,6) Q(i,7)]';    % rad/sec
    % desired angular velocity
    wd = [0 0 n]';                  % rad/sec
    % angular velocity error
    we = w - wd;                    % rad/sec
    % skew symmetric w
    ws = [0 -Q(i,7) Q(i,6);
        Q(i,7) 0 -Q(i,5);
        -Q(i,6) Q(i,5) 0];

    % gravity gradient torque
    M1(i) = (myu/Rc^3)*((6+10*phi(i))*(J3-J2)*(Q(i,2)*Q(i,3) ...
    + Q(i,1)*Q(i,4))*(1-2*(Q(i,1)*Q(i,1) + Q(i,2)*Q(i,2))) ...
    + 5*xi(i)*(2/5*J1*(Q(i,1)*Q(i,2)+Q(i,3)*Q(i,4)) ...
    + (J1-J3+J2)*(Q(i,1)*Q(i,2)-Q(i,3)*Q(i,4)) ...
    *(1-2*Q(i,1)*Q(i,1)+Q(i,2)*Q(i,2))) ...
```

```
    - 2* (J3-J2+J1)*(Q(i,1)*Q(i,3)+Q(i,2)*Q(i,4)) ...
    *(Q(i,3)*Q(i,2)+Q(i,1)*Q(i,4)));
    M2(i) = (myu/Rc^3)*((6+10*phi(i))*(J1-J3)*(Q(i,1)*Q(i,3) ...
    - Q(i,2)*Q(i,4))*(1-2*(Q(i,1)*Q(i,1) + Q(i,2)*Q(i,2))) ...
    + 5/2*xi(i)*(2/5*J2*(1-2*(Q(i,1)*Q(i,1)+Q(i,3)*Q(i,3))) ...
    + 4*(J2-J1+J3)*(Q(i,1)*Q(i,3)+Q(i,2)*Q(i,4)) ...
    *(Q(i,1)*Q(i,3)-Q(i,2)*Q(i,4)) ...
    - (J2-J3+J1)*(1-2*(Q(i,2)*Q(i,2)+Q(i,3)*Q(i,3))) ...
    *(1-2*(Q(i,1)*Q(i,1)+Q(i,2)*Q(i,2)))));
    M3(i) = (myu/Rc^3)*((12+20*phi(i))*(J2-J1)*(Q(i,1)*Q(i,3) ...
    - Q(i,2)*Q(i,4))*(Q(i,2)*Q(i,3)+Q(i,1)*Q(i,4)) ...
    + 5*xi(i)*(2/5*J3*(Q(i,2)*Q(i,3)-Q(i,1)*Q(i,4)) ...
    - 2*(J2-J1+J3)*(Q(i,1)*Q(i,2)-Q(i,3)*Q(i,4))...
    *(Q(i,1)*Q(i,3)-Q(i,2)*Q(i,4)) ...
    + (J1-J2+J3)*(1-2*(Q(i,2)*Q(i,2)+Q(i,3)*Q(i,3))) ...
    *(Q(i,2)*Q(i,3)+Q(i,1)*Q(i,4))));

    % gravity gradient torque
    M(1,i) = M1(i);
    M(2,i) = M2(i);
    M(3,i) = M3(i);
    %% Compute the control torque, tau
    tau(:,i) = -k*J*qe - c*J*we + ws*J*w - M(:,i);
    % each component of tau
    t1(i) = tau(1,i);
    t2(i) = tau(2,i);
    t3(i) = tau(3,i);

end
```

```

%% plot
subplot(311)
plot(t,t1)
xlabel('Time (sec)')
ylabel('\tau_x (Nm)')
subplot(312)
plot(t,t2)
xlabel('Time (sec)')
ylabel('\tau_y (Nm)')
subplot(313)
plot(t,t3)
xlabel('Time (sec)')
ylabel('\tau_z (Nm)')
```

Bibliography

[1] B. G. Williams D. J. Scheeres and J. K. Miller. Evaluation of the Dynamic Environment of an Asteroid: Applications to 433 Eros. *Journal of Guidance, Control, and Dynamics*, 23(3):466–475, May-June 2000.

[2] R. S. Hudson E. M. Dejong D. J. Scheeres, S. J. Ostro and S. Suzuki. Dynamics of Orbits Close to Asteroid 4179 Toutatis. *ICARUS*, 132.

[3] J.-P. Barriot S. R. Chesley D. W. Dunham R. W. Farquhar J. D. Giorgini C. E. Helfrich A. S. Konopliv J. V. McAdams J. K. Miller W. M. Owen Jr. D. J. Scheeres P. C. Thomas J. Veverka D. K. Yeomans, P. G. Antreasian and B. G. Williams. Radio Science Results During the NEAR-Shoemaker Spacecraft Rendezvous with Eros. *Science*, 289(5487):2085–2088, September 2000.

[4] W. Hu and D. J. Scheeres. Spacecraft Motion About Slowly Rotating Asteroids. *Journal of Guidance, Control, and Dynamics*, 25(4):765–775, July-August 2002.

[5] D. J. Scheeres J. K. Miller and D. K. Yeomans. The Orbital Dynamics Environment of 433 Eros:A Case Study for Future Asteroid Missions. *InterPlanetary Network Progress Report*, 42(152):1–26, February 2003.

[6] S. B. Broschart J. M. Mondelo and B. F. Villac. Dynamical Analysis of 1:1 Resonances near Asteroids: Application to Vesta. *Astrodynamics Specialist Conference*.

[7] JAXA. Current Status of the Asteroid Explorer HAYABUSA - Firing ion engine and starting second phase orbit maneuver to return to Earth, February 2009.

[8] Jet Propulsion Laboratory. JPL Small-Body Database, August 2003.

[9] A. K. Misra and Y. Panchenko. Attitude Dynamics of Satellites Orbiting an Asteroid. *The Journal of the Astronautical Sciences*, 54(3):369–381, July-December 2006.

[10] NASA. President Outlines Exploration Goals, April 2010.

[11] R. Nemiroff. Astronomy Picture of the Day, June 2001.

[12] D. J. Scheeres. The Orbital Dynamics Environment of 433 Eros. *ISTS*, 1.

[13] S. H. Strogatz. *Nonlinear Dynamics and Chaos*. Westview Press.

[14] M. Utashima. Spacecraft Orbits Around Asteroids for Global Mapping. *Journal of Spacecraft and Rockets*, 34(2):226–232, March-April 1997.

[15] B. Wie. *Space Vehicle Dynamics and Control*. AIAA Education Series.